Influence of Nutrient Gradient on Phytoplankton Size Structure, Primary Production and Carbon Transfer Pathway in a Highly Productive Area (SE Mediterranean)

Oumayma Chkili, Marouan Meddeb, Kaouther Mejri Kousri, Sondes Melliti Ben Garali, Nouha Makhlouf Belkhahia, Marc Tedetti, Marc Pagano, Amel Belaaj Zouari, Malika Belhassen, Nathalie Niquil, et al.

Ocean Science Journal (2023) 58:6
https://doi.org/10.1007/s12601-023-00101-6
Online ISSN 2005-7172
Print ISSN 1738-5261

Influence of nutrient gradient on phytoplankton size structure, primary production and carbon transfer pathway in a highly productive area (SE Mediterranean)

Oumayma Chkili[1,2,5] · Marouan Meddeb[1,2] · Kaouther Mejri Kousri[1,4] · Sondes Melliti Ben Garali[1,2] · Nouha Makhlouf Belkhahia[2] · Marc Tedetti[3] · Marc Pagano[3] · Amel Belaaj Zouari[4] · Malika Belhassen[4] · Nathalie Niquil[5] · Asma Sakka Hlaili[1,2*]

✉ Asma Sakka Hlaili
asma.sakkahlaili@gmail.com

[1] Université de Carthage, Faculté des Sciences de Bizerte, Laboratoire de Biologie Végétale et Phytoplanctonologie, Bizerte, Tunisie

[2] Université de Tunis El Manar, Faculté des Sciences de Tunis, Laboratoire des Sciences de l'Environnement, Biologie et Physiologie des Organismes Aquatiques LR18ES41, Tunis, Tunisie

[3] Aix Marseille Univ., Université de Toulon, CNRS, IRD, MIO UM 110, 13288 Marseille, France

[4] Institut National des Sciences et Technologies de la Mer (INSTM); 28, rue 2 mars 1934, Salammbô 2025, Tunisia

[5] CNRS, Normandie Université, UNICAEN, UMR BOREA (MNHN, CNRS-8067, Sorbonne Universités, Université Caen Normandie, IRD-207, Université des Antilles), CS 14032, Caen, France

Received: 16 July 2022 / Revised: 30 November 2022 / Accepted: 5 December 2022

Ocean Science Journal (2023) 58:6
https://doi.org/10.1007/s12601-023-00101-6
Online ISSN 2005-7172
Print ISSN 1738-5261

ABSTRACT

We assessed the spatial variability in the size structure of phytoplankton, community composition, primary production and carbon fluxes through the planktonic food web of the Gulf of Gabès (GG; Southeastern Mediterranean Sea) in the fall of 2017 during the MERMEX-MERITE cruise. High concentrations in nutrients, chlorophyll *a* (~2-6 µg L^{-1}) and primary production (1816-3674 mg C m^{-2} d^{-1}) revealed an eutrophic status of the studied stations in the GG. In accordance with hydrodynamic features, inorganic nutrients showed increases in concentrations from North to South and from coast to offshore, these nutrient gradients impacting the spatial distribution of phytoplankton community. Size-fractioned phytoplankton biomass and production were the lowest in the northernmost zone where they were mainly sustained by pico-sized fraction. Concomitantly, in this area, small aloricate ciliates were dominant leading to a high microbivory. Conversely, higher biomass and production were measured towards the South and offshore with prevalence of larger phytoplankton (nano- and/or micro-sized fractions) supported by diatoms. The herbivorous protozooplankton and metazooplankton were more abundant in these zones, resulting in an increase of the herbivory. The vertical particulate organic carbon flux followed also a north-south and coast-offshore increasing gradient, with a higher contribution of phytoplankton, and zooplankton fecal pellets to the sinking organic matter in the southernmost area. Our results suggest that even in nutrient-rich and highly productive waters, a continuum of trophic pathways, ranging from microbial to multivorous and herbivorous food webs, may exist, which implies different efficiencies in carbon export and carrying capacity within the ecosystem.

Keywords Phytoplankton size-structure · Primary production · Zooplankton grazing · Planktonic food web · Mediterranean Gulf

Online ISSN 2005-7172
Print ISSN 1738-5261

1 Introduction

The phytoplankton, through its biomass, diversity and productivity, has a key role in the functioning of marine ecosystems. The size structure of phytoplankton is an important planktonic trait that affects the magnitude of primary production, controls the size of grazers and hence regulates the carbon transfer through the marine food web (Decembrini et al. 2009; Ward et al. 2012; Sakka Hlaili et al. 2014; Negrete-García et al. 2022). Any shift in the size of phytoplankton may largely influence the planktonic food web dynamics and the overall efficiency of the marine system to export primary production (Legendre and Le Fèvre 1989; Legendre and Rassoulzadegan 1996).

In general, large phytoplankton (mainly micro-sized cells) is consumed by herbivorous zooplankton (mainly copepods), and primary production is efficiently transferred to higher consumers through the herbivorous food web. At the opposite, small phytoplankton (mainly pico-sized cells) and microbivorous protozooplankton (heterotrophic nanoflagellates and aloricate ciliates) are involved in the microbial food web that channels less carbon to higher consumers, as most of primary production is remineralized in the euphotic zone (Legendre and Le Fèvre 1989; Meddeb et al. 2018). More complex carbon pathways may be present in marine ecosystems. The multivorous food web, in which large and small phytoplankton, as well as herbivorous and microbivorous zooplankton play all together significant roles, can be efficient in carbon transfer (Legendre and Rassoulzadegan 1995). The bacterial-multivorous food web, in which phytoplankton and bacterioplankton contribute together to carbon production, was recently identified and reported to be less efficient in carbon transfer because of the recycling of the latter (Meddeb et al. 2019). Legendre and Rassoulzadegan (1995) reported that the dynamics of planktonic food web was related to that of nutrients and thus described a continuum of trophic pathways between eutrophic and oligotrophic systems, going from herbivorous to multivorous and microbial food webs.

Online ISSN 2005-7172
Print ISSN 1738-5261

The nutrient conditions are controlled by physical processes that ultimately influence the size structure of phytoplankton and the primary production (Estrada et al. 1999; Cermeño et al. 2006; Ferland et al. 2011). Previous studies in the Mediterranean Sea have shown that trophic status driven by hydrodynamic forcing can impact the structure of food webs and promote the ecosystem's ability to export biogenic carbon. In highly stratified oligotrophic open waters, where primary production is low, pico- and nano-sized cells dominate the phytoplankton community (Decembrini et al. 2009). Most carbon is then channeled to higher consumers through microbial food web, with a high recycling activity (Giannakourou et al. 2014; Livanou et al. 2019). Changes in the food web structure can occur when vertical deep mixing or upwelling supply nutrients to the euphotic zone that promote large-sized phytoplankton (i.e., diatoms) and substantially increase primary production (Allen et al. 2002). In that case, the food web shifts to an herbivorous pathway that efficiently transfers carbon to upper trophic levels (Stibor et al. 2019).

In the Mediterranean coastal systems, hydrodynamic features (mesoscale structures, tides…) may influence the hydrological and biogeochemical parameters (salinity, temperature, nutrients…) that finally impact the size structure and composition of phytoplankton (Caroppo et al. 2006, 2018; Geyer et al. 2018; Trombetta et al. 2021). Decembrini et al. (2020) have recently shown that the lateral advection of nutrient-rich water in the Gulf of Augusta (Eastern Sicilian coast, Ionian Sea) triggered a change in the size structure of phytoplankton and primary production with a significant ecological effect on the planktonic food web. Besides physical forcing, continental nutrient inputs from anthropogenic activities can influence the phytoplankton structure and alter the relationship between the latter and grazers, with possible changes in trophic pathways (Smith et al. 2006; Decembrini et al. 2021). The coastal Mediterranean environments are typically mesotrophic or eutrophic systems, with relatively high nutrient concentrations and dominance of large-sized phytoplankton (MedECC 2020). Yet, the herbivorous food web is not usually observed and other trophic pathways (such as

Online ISSN 2005-7172
Print ISSN 1738-5261

microbial or multivorous food webs) can occur at spatial and seasonal scales (Grami et al. 2008; Meddeb et al. 2018; Decembrini et al. 2021; Trombetta et al. 2022), probably due to the influence of the hydrological properties of the system. Therefore, the interactions between hydrodynamics and nutrient inputs must be taken into account to describe the structure of marine food web in eutrophic coastal ecosystems (Liu et al. 2018; Decembrini et al. 2021).

Although much interest has been given to primary production and its trophic transfer in the Mediterranean Sea (Moran and Estrada 2001; Casotti et al. 2003; Psarra et al. 2005; Decembrini et al. 2009; Kovač et al. 2018; Mayot et al. 2020), data acquired in its Southern basin are scarce (Sakka Hlaili et al. 2008; Grami et al. 2008; Meddeb et al. 2018). Furthermore, little effort has been dedicated to describe how nutrient inputs and physical features affect the phytoplankton community structure and food web dynamics. In the Southeastern Mediterranean Sea, the Gulf of Gabès (hereafter refers to as GG) is a highly dynamical coastal ecosystem, characterized by a large continental shelf with relatively shallow well-mixed and rich-nutrient waters (Bel Hassen et al. 2009; Zayen et al. 2020), which is in contrast to the oligotrophic status of the Eastern Mediterranean basin. The nutrient enrichment results mainly from the anthropogenic inputs (mostly by phosphoric acid industries) (Khedhri et al. 2014; El Kateb et al. 2018) and the atmospheric deposition through Saharan dust (Khammeri et al. 2018) . The GG is also characterized by a complex water circulation, which results from the combination of the general thermohaline circulation (Bel Hassen et al. 2009), the anticyclonic winds and the strong tides (Sammari et al., 2006, Hattour et al. 2010; Othmani et al. 2017) (see details below). This circulation induces North-South and coast-offshore transports, which induce a gradient of particles and dissolved elements (such as nutrients) with accumulation in the Southern part of the GG (Ciglenečki et al. 2020; Mansouri et al. 2020). Previous studies have actually shown that phytoplankton dynamics within the GG was related to the nutrient conditions and water physical properties (Bel Hassen et al. 2008, 2009; Drira et al. 2009, 2014). Spatial distributions were also documented for protozooplankton and copepod communities and were shown to be

Online ISSN 2005-7172
Print ISSN 1738-5261

linked to the combination of hydrodynamic conditions and anthropogenic loads (Hannachi et al. 2008; Drira et al. 2009, 2017; Makhlouf Belkahia et al. 2021). Although nutrient inputs and water circulation are recognized as major drivers in influencing the dynamics of phytoplankton and zooplankton in the GG (Béjaoui et al. 2019), the link between these communities and their functional roles are not well known.

The aim of this study is to analyze the size structure of phytoplankton and the size-fractionated primary production, as well as trophic interactions between planktonic components in order to define the main characteristics of carbon transfer pathway. In particular, our work aims to demonstrate how food web structure changes along a nutrients spatial gradient in a highly dynamical environment like the GG. The study will also allow verifying whether the "continuum of trophic pathways" reported by Legendre and Rassoulzadegan (1995) could be found in highly productive waters characterized by a gradient of eutrophic conditions.

2 Materials and Methods

2.1 Hydrodynamic features of the study area

The GG is a relatively shallow ecosystem which is strongly influenced by hydrodynamic forcing, mainly driven by the general Mediterranean circulation, the anticyclonic winds and the high tide effects (Hattour et al. 2010; Othmani et al. 2017). The Atlantic Tunisian Current (ATC) is a surface current originating from the Atlantic Ocean. It crosses the Sicilian-Tunisian Channel, flows along the Tunisian continental shelf southward, and splits into two branches (Fig. 1). One coastal branch of the ATC enters the GG and creates an anticyclonic circulation in its Southern part (Ben Ismail et al. 2012; Boukthir et al. 2019). The other branch flows on southeastward along the Libyan shelf, giving rise to the Atlantic Libyan Current (ALC) (Ben Ismail et al. 2015). Furthermore, the hydrodynamics of the GG is deeply influenced by barometric tides (Sammari et al. 2006), which have the highest range of the Mediterranean Sea with a maximal amplitude (~ 2 m) in the Southern region (Abdennadher and Boukthir 2006;

Online ISSN 2005-7172
Print ISSN 1738-5261

159 Othmani et al. 2017). Concomitantly with our work, Zayen et al. (2020) investigated the
160 hydrodynamic circulation in the GG, and reported an average littoral current flowing North to
161 South and two eddies in the middle of the GG that induce a counter current on the littoral in its
162 Southern part (Fig. 1).

163

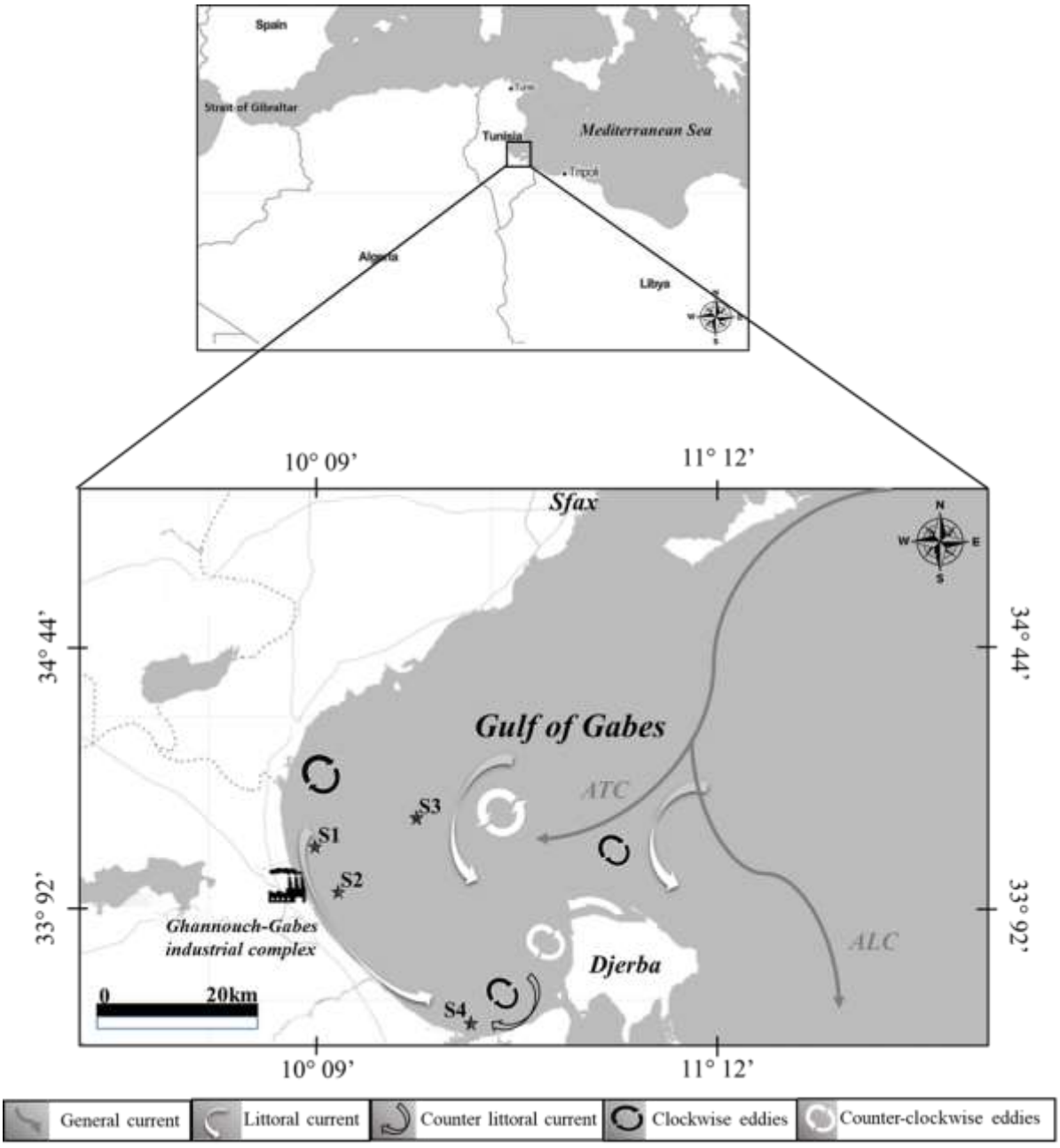

164

165 **Fig. 1** Gulf of Gabès: localization of the sampling stations and hydrodynamic circulation
166 (Atlantic Tunisian Current: ATC and Atlantic Lybian Current: ALC). Modified from Zayen et
167 al. (2020)

168

Online ISSN 2005-7172
Print ISSN 1738-5261

169 **2.2 Choice of study stations and sampling**

170 The study was carried out within the framework of the MERMEX-MERITE project
171 (*Marine Ecosystems Responses In The Mediterranean Experiment)* campaign from 31 Oct. to
172 3 Nov. 2017. We investigated the overall function of plankton communities based on sampling
173 and field experiments carried out simultaneously, which was not easy to achieve in several
174 stations. Therefore, to meet our objective, we chose to explore several key processes in plankton
175 communities in four relevant stations within the GG (S1, S2, S3 and S4; Fig. 1). The choice of
176 the stations was based on a preliminary work emphasizing a heterogeneous distribution of
177 nutrients in the study region, with increased concentrations from North to South and from the
178 coast to offshore (Fig. S1 in Supplementary Material).

179 Station S2 was located in front of the phosphoric acid plant of the Ghannouch-Gabès
180 industrial complex and was chosen as to represent coastal waters impacted by phosphogypsum
181 loading; Stations S1 and S4 were located on either side of station S2 (North and South,
182 respectively), while S3 was an offshore station in front of S1 (Fig. 1). The characteristics of the
183 stations and sampling are reported in Table 1.

184 In each station, seawater was collected using 2.5 L plastic water sampler (Hydro-Bios),
185 and water temperature, salinity, pH and dissolved oxygen (O_2) were measured *in situ* with a
186 multi-probe sensor (Multi 1970i, WTW) at three depths (between 0.5 and 14 m) depending on
187 the maximal water depth of the stations (Table 1). The collected water was filtered through a
188 200 µm mesh screen to remove large zooplankton, and three subsamples from each depth were
189 taken for nutrients, chlorophyll *a* (Chl *a*), phytoplankton and protozooplankton analyses. At
190 each station, metazooplankton (> 200 µm organisms) was collected with a 28 cm diameter
191 WP2 200 µm net by vertical hauls from the bottom to the surface. A flow meter was used to
192 determine the water volume filtered during the net tow.
193
194

Online ISSN 2005-7172
Print ISSN 1738-5261

Table 1 Main characteristics, environmental parameters and phytoplankton biomasses of the sampling stations within the Gulf of Gabès during the fall 2017. Physico-chemical variables and Chl *a* concentrations are depth-averaged values; carbon biomasses are depth-integrated values (Mean value ± SD, N = 9). p-value (ns: not significant; *: 0.01 < p < 0.05; ** 0.001 < p < 0.01, ***: p < 0.001) indicates the significant level for the ANOVA used to test spatial variation

		S1	S2	S3	S4	p-value
Coordinates	Latitude (N)	34° 01.767'	33° 56.545'	34° 01.491'	33° 52.346'	
	Longitude (E)	10° 06.295'	10° 08.939'	10° 19.940'	10° 11.803'	
Sampling date		30/10	01/11	01/11	03/11	
Tide condition / height (m)		High / 1.6	High / 1.9	Low / 0.7	Low / 0.8	
Maximum water depth (m)		13.5	12.1	18.8	13.6	
Sampled depths (m)		0.5; 2.5; 5	2.5; 4; 7	2; 8; 14	2; 6; 10	
Water temperature (°C)		22.55 ± 0.64	22.90 ± 0.37	22.89 ± 0.21	24.18 ± 0.52	ns
Salinity		39.43± 0.85	39.56± 0.37	39.48± 0.25	39.42± 0.54	ns
pH		8.31 ± 0.005	8.24 ± 0.028	8.27 ± 0.01	8.25 ± 0.017	ns
Dissolved O_2 (mg L^{-1})		8.20 ± 0.05	8.25 ± 0.02	8.23 ± 0.04	8.15 ± 0.11	ns
N_{inorg} (µM)		4.27 ± 0.36	7.63 ± 0.43	5.12 ± 0.31	8.93 ± 2.11	*
N_{org} (µM)		12.29 ±2.42	9.20 ± 0.27	6.50 ± 0.11	5.03 ± 0.49	**
P_{inorg} (µM)		0.91 ± 0.27	1.77 ± 0.44	1.52 ± 0.08	2.20 ± 0.05	*
P_{org} (µM)		8.23 ± 1.93	16.95 ± 2.42	11.45 ± 0.18	18.32 ± 0.02	***
$Si(OH)_4$ (µM)		4.90 ± 0.22	5.34 ± 0.40	6.40 ± 0.30	8.98 ± 0.76	***
Chl *a* (µg L^{-1})		1.65 ± 0.06	3.68 ± 1.63	5.90 ± 1.12	6.06 ± 0.24	**
% of total Chl *a*						
Microphyt.		35 ± 3	30 ± 2	49 ± 5	74 ± 5	***
Nanophyt.		28 ± 5	43 ± 6	30 ± 4	15 ± 5	*
Picophyt.		37 ± 6	27 ± 5	21 ± 4	11 ± 1	ns
Carbon biomass (mg C m^{-2})		780.22 ± 65.60	854.50 ± 90.19	1300.3 ± 44.28	1624.57 ± 134.80	**
Microphyt.		418 ± 51 (54%)	608 ± 91 (71%)	951 ± 30 (74%)	1207 ± 30 (75%)	***
Nanophyt.		265 ± 14 (9%)	72 ± 0.4 (8%)	86 ± 13 (7%)	265 ± 13 (16%)	***
Picophyt.		152 ± 0.1 (38%)	175 ± 0.1 (21%)	263 ± 0.1 (20%)	152 ± 0.1 (9%)	**

2.3 Nutrient, Chl *a* and plankton analyses

Inorganic nitrogen (N_{inorg}: NO_2^- + NO_3^- + NH_4^+), inorganic phosphorus (P_{inorg}: PO_4^{3-}) and silicates ($Si(OH)_4$), as well as total nitrogen (N_{total}) and phosphorus (P_{total}) were analyzed with a BRAN and LUEBBE type 3 autoanalyzer (Bran + Luebbe Co, Germany). The precision for all nutrient analyses was ≤ 1%. Organic nutrients (N_{org} and P_{org}) were estimated as the difference between total and inorganic elements.

Online ISSN 2005-7172
Print ISSN 1738-5261

For Chl *a* analysis, water samples (1 L) were successively filtered through 10, 2 and 0.2 µm polycarbonate membranes to determine size-fractionated Chl *a* (> 10, 2-10 and ≤ 2 µm). Filtrations were performed under low vacuum pressure (< 100 mm Hg) and low light intensity. Chl *a* concentrations were estimated using the spectrophotometric method after 24 h extraction in 90% acetone at 4 °C in the dark (Parsons et al. 1984). Total Chl *a* concentration was estimated as the sum of the three size-fractioned Chl *a* concentrations.

To enumerate picophytoplankton (≤ 2 µm cells), 2 mL samples were immediately fixed after sampling with 20% paraformaldehyde solution, then placed at 4 ºC in the dark for 15 min, and finally frozen at -80 ºC in liquid nitrogen until analysis with a CyFlow® Space flow cytometer (Partec). Prior to analysis, the samples were filtered on 30 µm pore size filters and enriched with fluorescent beads of 1 and 2 µm in diameter (Polysciences, Inc) as internal cell size standards. Trucount™ beads were also added to accurately estimate the volume of each sample (BD-Biosciences). Picoprokaryotes and picoeukaryotes were identified and counted on the basis of their relative forward scatter (FSC) and phycoerythrin orange fluorescence (at 488 nm) and Chl *a* red fluorescence (at 638 nm), respectively. Cell volumes were determined using equivalent diameters estimated from flow cytometry. The biovolumes (picoprokaryotes: 1.77 μm^3; picoeukaryotes: 4.19 μm^3) were converted into carbon content using the following conversions: 0.357 pg C μm^{-3} for picoprokaryotes, and 0.433 x $(\mu m^3)^{0.863}$ for picoeukaryotes (Verity et al. 1992). The cell carbon contents were multiplied by the abundances to estimate the carbon biomass of picophytoplankton (mg C m^{-3}). Depth-integrated biomass (mg C m^{-2}) was obtained from the carbon biomasses estimated for the three depths.

Phytoplankton samples (nano-: 2-10 µm; micro-phytoplankton: > 10 µm) were preserved in 3% acidic Lugol's solution and stored at room temperature in the dark (Parsons et al. 1984). The identification and counting of cells (at least 500 *per* sample) were determined using the Motic AE31E inverted microscope on 100 mL settled volume (Utermöhl 1931; Lund et al. 1958). Cell dimensions of phytoplankton taxa were measured using a calibrated ocular

Online ISSN 2005-7172
Print ISSN 1738-5261

micrometer and biovolumes were determined by applying standard geometric formulae to each taxon (Hillebrand et al. 1999). Then, the biovolumes were converted into carbon content using specific conversion factors or formulae (Putt and Stoecker 1989; Menden-Deuer and Lessard 2000) for diatoms, autotrophic flagellates and ciliates, as detailed in Meddeb et al. (2018). The carbon biomass of phytoplankton (mg C m^{-3}) was then determined by multiplying the carbon content of different taxa by their specific abundances. Carbon biomasses from the three sampled depths were used to calculate the depth-integrated biomass (mg C m^{-2}).

Protozooplankton samples (100 mL) were fixed with 4% basic Lugol's solution (Sherr and Sherr 1993), and organisms were identified and counted (at least 200 cells *per* sample) according to the inverted microscopy technique of Utermöhl (1931). Protozooplankton was composed of heterotrophic nanoflagellates and ciliates including loricate and aloricate species, but also of dinoflagellates (most of which are phagotrophic). Within dinoflagellates, mixotrophic and heterotrophic organisms were distinguished according to several works (Sakka Hlaili et al. 2007; Jeong et al. 2010; Boutrup et al. 2016). The ebridian flagellate *Hermesinium sp.* was also considered as a micrograzer since its mixotrophy had been confirmed (Hargraves 2002; Jafari et al. 2015).

Samples of metazooplankton (250 mL) were fixed with a 5% borate-buffered formalin solution. Metazoan organisms were counted and identified in the whole sample using a Leica M 205C stereo microscope.

2.4 *In situ* dilution experiment

The dilution method (Landry and Hassett 1982) was used to estimate the growth rate of phytoplankton and its grazing rate by protozooplankton at each station and at the same sampling date. Water samples were collected over the water column (5 m for S1, 7 m for S2, 14 m for S3 and 10 m for S4) with a submersible pump and then filtered through 200 µm mesh screen (to remove meso- and macroplankton). This screened seawater was diluted with free-particle seawater to achieve four dilutions (25, 50, 75 and 100% of 200 µm screened seawater). The

Online ISSN 2005-7172
Print ISSN 1738-5261

diluting seawater was obtained by gravity filtration using a 0.22 µm sterile filter capsule (polycap 75 AS). Triplicate 2 L polycarbonate bottles (Nalgene®) were used for each dilution, and all bottles were incubated *in situ* for one day (t = 1 d). The GG is a nutrient-rich environment where nutrients are considered as available throughout the year (Bel Hassen et al. 2008; Béjaoui et al. 2019). Therefore, nutrients were not added to our dilution bottles to avoid the overestimation of growth rates. Furthermore, several authors have found that growth rates in nutrient-enriched bottles were not significantly different from those estimated without nutrients during dilution experiments conducted in nutrient-rich systems (Olson and Strom 2002; Sakka Hlaili et al. 2007; Pecqueur et al. 2022). Subsamples were taken from each dilution bottle at the beginning and the end of incubation to determine initial and final phytoplankton carbon biomasses (C_0 and C_t ; respectively). As protozoans have a prey size-selective feeding activity (Sakka Hlaili et al. 2007; Zhang et al. 2017), size-fractioned biomass of phytoplankton was determined (i.e., pico-: ≤ 2 µm, nano-: 2-10 µm, and microphytoplankton: > 10 µm). The apparent growth rate of each size fraction prey (R) was calculated from the changes in carbon biomass during the incubation period as:

$$R(d^{-1}) = \ln\left({C_t}/{C_0}\right) \times t^{-1}$$

The coefficients R were plotted against the dilution factor, and a model I linear regression was used to estimate growth rates k (d^{-1}) (i.e., the y-intercept that represented growth in 100% dilution in the absence of grazers) and the grazing coefficient g (d^{-1}) (i.e., the slope of the regression line) (Landry and Hassett 1982). For each size fraction in all stations, the regression lines were tested as significant by Student's t-test ($p < 0.05$) and were represented in the Supplementary Material (Fig. S2).

For each phytoplankton size fraction, production rates (P_1) and consumption rates by protozooplankton (G_{p1}) were calculated according to several authors (Grattepanche et al. 2011; Meddeb et al. 2018) as:

Online ISSN 2005-7172
Print ISSN 1738-5261

$$P_1\,(mg\ C\ m^{-3}\ d^{-1}) = k \times C_0\left[e^{(k-g)t} - 1\right]/(k - g \times t)$$

and

$$G_{p1}\,(mg\ C\ m^{-3}\ d^{-1}) = g \times C_0\left[e^{(k-g)t} - 1\right]/(k - g \times t)$$

The P_1 and G_{p1} data were multiplied by the sampling depth to get depth-integrated rates of production (P, mg C m^2 d^{-1}) and consumption (G_p, mg C m^2 d^{-1}), respectively. Depth-integrated production rates for the three size fractions were added to obtain production rate for total phytoplankton. The percentage of production consumed *per* day was estimated as:

$$\%Pgrazed\ d^{-1} = \left({}^{G_p}/_{P}\right) \times 100$$

2.5 Metazooplankton gut fluorescence analysis

The grazing of metazooplankton on phytoplankton was estimated using the gut fluorescence method (Slaughter et al., 2006). Zooplankton was collected as indicated above. To account for vertical migration of zooplankton likely to affect its feeding activity, sampling was carried out around sunset, when zooplankton perform a vertical ascension. Three 500 mL subsamples of the cod content were immediately narcotized with 10% carbonated water (final concentration, v/v) to minimize stress and gut evacuation by zooplankton (Kleppel and Pieper 1984) and were kept frozen in the dark to minimize fecal pellet production by the organisms (Saiz et al. 1992). The zooplankton subsamples were thawed and washed with filtered seawater to remove adhering algae and debris, and filtered onto 47 mm diameter GF/F membranes that were extracted in 10 mL of 90% acetone solution maintained at 4 °C in the dark. After overnight extraction, each solution was centrifuged, and the supernatant absorbance was measured using a Jenway spectrophotometer before and after acidification with 10% hydrochloric acid solution (Parsons et al. 1984).

The gut pigment content (GP) was calculated according to Slaughter et al. (2006) as:

$$GP(mg\ pigment\ m^{-3}) = (GP_{sub} \times v)/(F \times V_{net}),$$

Online ISSN 2005-7172
Print ISSN 1738-5261

where GP_{sub} (mg pigment m^{-3}) is the phaeopigment concentration in the subsample, v (m^3) is the volume of the subsample, F is the fraction of subsample processed for gut pigment content, and V_{net} (m^3) is the total volume of seawater filtered during the net tow.

Consumption of > 2-µm phytoplankton by metazooplankton was calculated as:

$$G_m(mg\ C\ m^{-2}\ d^{-1}) = [GP \times CR \times C{:}Chla] \times D,$$

where D is the depth of the net tow (m), C:Chl *a* is the depth-averaged C:Chl *a* ratio determined for > 2 µm phytoplankton at each station, and CR is the gut clearance rate of metazooplankton (d^{-1}). The CR was obtained from the gut clearance rate constant (GCRC) *vs.* temperature (T) relationship (GCRC = 0.0117 + 0.001794T) (Dam and Peterson 1988; Irigoien 1998; Mauchline 1998).

The impact of metazooplankton grazing on the standing stock and production of phytoplankton were calculated as:

$$\%Chla\ grazed\ d^{-1} = (GP \times CR \times 100)/SC$$

$$\%P\ grazed\ d^{-1} = \left({}^{G_m}/_{P}\right) \times 100,$$

where SC is the depth-averaged concentration of Chl *a* and P is the production rate of nano- and micro-phytoplankton, estimated by the dilution method.

2.6 Vertical carbon fluxes

Sediment traps were used to estimate the vertical flux of particles, including phytoplankton, metazooplankton fecal pellets, and detritus. This technique was performed by several authors (Laurenceau-Cornec et al. 2015; Xiang et al. 2022; Kojima et al. 2022) because it is very useful for estimating the particle sinking and gives details in the composition of the sinking fluxes. At each station, two sediment traps (63 cm high, 9 cm internal diameter) were incubated vertically two meters from the bottom. Prior to deployment, the traps were filled with dense seawater (0.2 µm filtered seawater + NaCl 5 g L^{-1}) to create a density gradient and avoid collecting surface particles. After 24 h incubation, the traps were closed *in situ*, returned to the laboratory and stored at 5 °C overnight to let particles settle. The supernatant was removed from

Online ISSN 2005-7172
Print ISSN 1738-5261

each trap and the bottom contents of the two traps were mixed. Subsamples were taken from the trapped material for further analyses of particulate organic carbon (POC), phytoplankton and fecal pellets.

For POC, ~ 500 mL seawater samples were filtered onto precombusted glass fiber filters (450 °C, 24 h) (Whatman GF/F, 25 mm). The filters were oven dried at 50 °C for 24 h and stored in clean glass vials in a desiccator. POC was determined by the high combustion method and mass spectrometry according to Raimbault et al. (2008).

Phytoplankton (> 2 µm cells) was enumerated on 500 mL subsamples fixed with acidic Lugol's solution (final concentration 4%), and cell abundances were converted into carbon biomasses as described above.

Subsamples (200 mL) were preserved in buffered formaldehyde (final concentration 7%) for counting fecal pellets using an inverted microscope (× 100 magnification). Differently shaped pellets were distinguished (cylindrical, conical; ovoid and round), and their dimensions were measured using a calibrated ocular micrometer.

The vertical fluxes of phytoplankton (F_{phyt}) and detritus (F_{det}) were estimated following Grami et al. (2008):

$$F_{phyt}(mg\ C\ m^{-2}d^{-1}) = {}^{1}/_{2}\left(C_{phyt} \times V_{tr}\right)/S_{tr} \times t$$

$$F_{det}(mg\ C\ m^{-2}d^{-1}) = {}^{1}/_{2}\left(C_{det} \times V_{tr}\right)/S_{tr} \times t,$$

where C_{phyt} is the carbon biomass of nano- and microphytoplankton (mg C m^{-3}) and C_{det} is the detrital carbon estimate, calculated as the POC concentration minus the carbon biomass of all particles. V_{tr} is the volume of trapped material (m^3), S_{tr} is the trap area (m^2) and t is the duration of incubation (d). The vertical flux of phytoplankton was considered to be the phytoplankton export from the planktonic system towards the benthos, while the vertical flux of detritus was assigned to the sinking flux.

Online ISSN 2005-7172
Print ISSN 1738-5261

The volume of each pellet shape category (V_{pel}, mm^3 m^{-3}) was estimated from its dimension and abundance. Then, its vertical volume flow (S_{pel}) and vertical carbon flux (F_{pel}) were estimated following Grami et al. (2008):

$$S_{pel}(mm^3 m^{-2} d^{-1}) = {}^1/_2 \left(V_{pel} \times V_{tr}\right)/S_{tr} \times t$$

$$F_{pel}(mg\ C\ m^{-2} d^{-1}) = S_{pel} \times f,$$

where f is a conversion factor (0.057 mg C mm^{-3} for cylindrical/conical pellets and 0.042 mg C mm^{-3} for ovoid/rounded pellets).

2.7 Statistical analyses

An analysis of variance (ANOVA) was used to test the significance of the spatial variation of physico-chemical factors, Chl *a*, plankton concentrations and vertical fluxes. ANOVA was also used to compare (i) environmental factors and plankton concentrations among depths, and (ii) the estimates of rates (k, g, P, G_p, G_m) between phytoplankton size fractions (> 10, 2-10 and < 2 µm) or stations. The assumptions of normality of data distribution (Kolmogorov-Smirnov test) and homogeneity of variance (Bartlett-Box test) were met. Spearman correlations (r_s) were used to test the relationships between different variables: phytoplankton (Chl *a*, carbon biomass, growth rate, production rate) and nutrients; growth (k) and grazing (g) rates; coefficients g and G_p and protozooplankotn abundances; production (P) and consumption rate by protozooplankton (G_p); consumption rate by metazooplankton (G_m) and phytoplankton biomass and metazoans abundances. ANOVA and correlation analyses were performed in SPSS software 18.0 for Windows.

Canonical correspondence analysis (CCA; Ter Braak 1986) was performed to relate the spatial distribution of plankton communities to environmental parameters (P_{org}, P_{inorg}, N_{inorg}, N_{org}, $Si(OH)_4$, pH, temperature and salinity). The CCA also elucidated the relationship between the biomass of size-fractioned phytoplankton and different zooplanktonic groups. Phytoplankton and zooplankton data were ln (x + 1) transformed. The comparison of the canonical inertia associated with the CCA (constrained ordination) and the inertia of the

Online ISSN 2005-7172
Print ISSN 1738-5261

classical correspondence analysis (CA, unconstrained ordination) indicated the extent to which the environmental variables explained the spatial structure of communities. Permutation tests (n = 999) were performed to identify the significant axis and to test the significance of the correlations between environmental factors and plankton distribution.

3 Results

3.1 Environmental conditions

Sampling stations were located in the continental shelf of the GG, which is characterized by a shallow (< 20 m) well-mixed water column. Environmental factors showed no significant variations between sampling depths (ANOVA $p > 0.05$), and hence data were presented as depth-averaged values (Table 1). Water temperature (22.6-24.2 °C), salinity (39.42-39.56), pH (8.25-8.31) and dissolved O_2 (8.15-8.25 mg L^{-1}) varied little among stations, while nutrient concentrations exhibited significant spatial variations (ANOVA, $p < 0.05$). In S1, inorganic nutrients presented the lowest values (4.27 µM N, 0.91 µM P and 4.90 µM Si) and increased up to 8.93 µM N, 2.2 µM P and 8.98 µM Si in S4. Inorganic nutrient concentrations recorded in S3 were higher than in S1, but lower than the southernmost station (S4). The highest and lowest levels of organic nitrogen (N_{org}: 5.03-12.29 µM) were recorded in S1 and S4, respectively. An opposite trend was observed for organic phosphorus (P_{org}: 8.23-18.32 µM).

3.2 Spatial distribution of planktonic communities

Phytoplankton. The depth-averaged Chl *a* concentrations and the depth-integrated carbon biomasses were different among stations (ANOVA, $p < 0.05$; Table 1), increasing gradually from S1 (1.7 µg Chl *a* L^{-1}, 780 mg C m^{-2}) to S4 (6.07 µg Chl *a* L^{-1}, 1,624 mg C m^{-2}). Positive correlations were found between inorganic N, P and Si and Chl *a* concentrations (r_s = 0.64-0.84, $p < 0.01$) and carbon biomass (r_s = 0.67-0.78, $p < 0.01$). Microphytoplankton was the main source of Chl *a* in S4 (74%) and contributed to ~50% of it in S3. The contribution

Online ISSN 2005-7172
Print ISSN 1738-5261

of picophytoplankton to Chl *a* was higher in S1 (37%) than in the other stations (11-27%), while nanophytoplankton contributed to a large fraction of Chl *a* in S2 (43%) (Table 1). In terms of carbon biomass, micro-sized fraction (418-1207 mg C m^{-2}) formed the most of phytoplankton (54-75%), while nano-sized fraction (70-265 mg C m^{-2}) contributed only by 9-16%. The pico-sized fraction (152-292 mg C m^{-2}), which formed only 9% of phytoplankton carbon in S4, showed increased contributions in S2 and S3 (20-21%) and mostly in S1 (38%).

The composition of > 2 µm phytoplankton community changed also among stations. Diatoms showed different contributions to the community according to the station, and their biomass was positively correlated with inorganic N, P and Si (r_s = 0.79-0.67, $p < 0.01$). Diatoms were dominant in S2, S3 and S4, showing depth-averaged contribution of 73-88% (Fig. 2a). They were mainly represented by *Leptocylindrus minimus* (30-60% of diatoms) in the three stations. Large chains of *Skeletonema costatum* and *Rhizosolenia setigera* showed increased contribution to diatoms (18-28%) only in S3 and S4 (Fig. 2b). The small phytoplagellates were particularly abundant in S1 (45%; Fig. 2a), and were represented by nano-sized Cryptophyceae (*Hillea fusiformis* and *Rhodomonas marina*). Within the phytoflagellates, the micro-sized Dictyochophyceae (i.e., *Dictyocha fibula*) were more important in S3 and S4 than in the other stations (Fig. 2c). In all stations, photosynthetic ciliates (*Mesodinium rubrum*) and dinoflagellates (*Prorocentrum gracile*) only accounted for 2-13% of the > 2 µm phytoplankton community (Fig. 2a).

Ocean Science Journal (2023) 58:6
https://doi.org/10.1007/s12601-023-00101-6
Online ISSN 2005-7172
Print ISSN 1738-5261

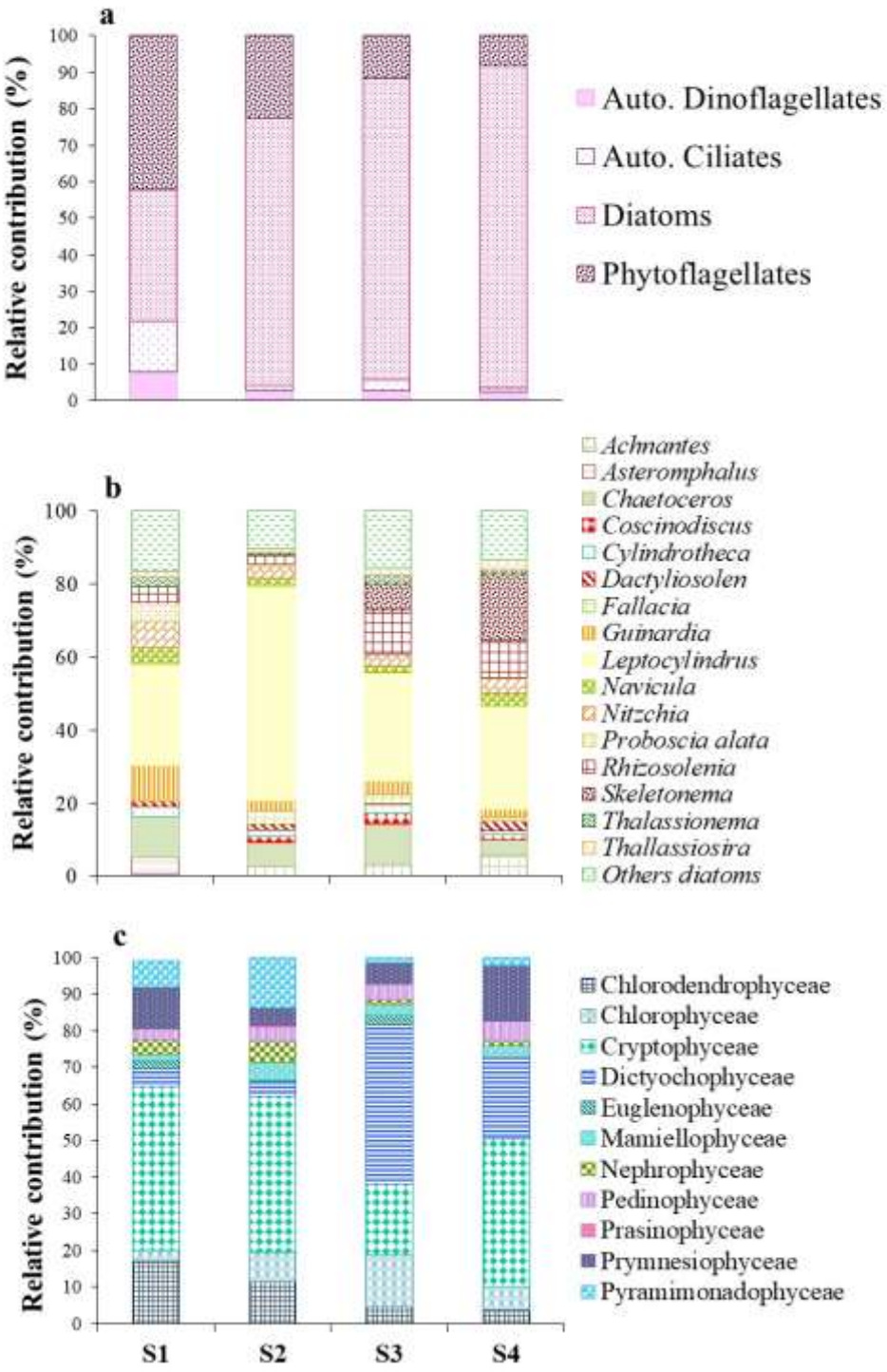

427

428 **Fig. 2** Composition of > 2 µm phytoplankton (**a**), diatoms (**b**) and phytoflagellates (**c**) in the
429 sampling stations during fall 2017. Values are the means of the three depths at each station.

430

Online ISSN 2005-7172
Print ISSN 1738-5261

Protozooplankton. The depth-averaged abundance of total protozooplankton was significantly different between stations (ANOVA, $p < 0.05$), varying from 43×10^3 cells L^{-1} (in S3) to 123×10^3 cells L^{-1} (in S1) (Fig. 3a). Aloricate ciliates, mainly composed of *Strombidium* spp. (Fig. 3b), were dominant in S1 (~60%; 70×10^3 cells L^{-1}). Loricate ciliates displayed a relatively low abundance (1.5-6 $\times 10^3$ cells L^{-1}) and were most abundant in S4, where *Tintinnopsis*, *Helicostomella* and *Amphorellopsis* occurred (Fig. 3b). Dinoflagellates were abundant in S2, S3 and S4 (20-55 $\times 10^3$ cells L^{-1}), contributing to 48-64% of protozooplankton. Mixotrophic dinoflagellates including *Gymnodinium*, *Heterocapsa*, *Karenia* and *Neoceratium* (Fig. 3c) were dominant in S2 (59% of dinoflagellates), whereas large heterotrophic dinoflagellates (mainly *Protoperidinium*) mostly occurred in S4 (60%). The heterotrophic nanoflagellate *Commation cryoporinum* (0.75-5.78 $\times 10^3$ cells L^{-1}) and the ebridian flagellate *Hermesinium sp.* (8.7-26.7 $\times 10^3$ cells L^{-1}) contributed 2-12% and 15-37% to protozooplankton, respectively (Fig. 3a).

Metazooplankton. Metazooplankton abundance significantly varied among stations (ANOVA, $p < 0.05$) from 11×10^2 ind. m^{-3} in S1 to 20×10^2 ind. m^{-3} in S4 (Fig. 4a). Copepods (7.5-12.5 $\times 10^2$ ind. m^{-3}) were dominant in all stations, forming 53-86% of total metazooplankton (Fig. 4a). Calanoida (*Centropages*, *Clausocalanus*, *Paracalanus* and *Phaenna*) and Cyclopoida (*Oithona*) contributed to the majority of copepods, but with different percentages according to the station (Fig. 4b). The harpacticoid *Euterpina* was relatively abundant in S3 (12%). Cladocerans (*Penilia sp.*) mainly occurred in S4 (forming 16% of metazoans), while decapod, polychaete and crab larvae as well as, crustacean nauplii were observed at moderate concentrations in S2, S3 and S4. Other metazoan groups, e.g., chaetognaths, appendicularians, nematodes and siphonophores were observed in all stations, but at much lower densities.

Ocean Science Journal (2023) 58:6
https://doi.org/10.1007/s12601-023-00101-6
Online ISSN 2005-7172
Print ISSN 1738-5261

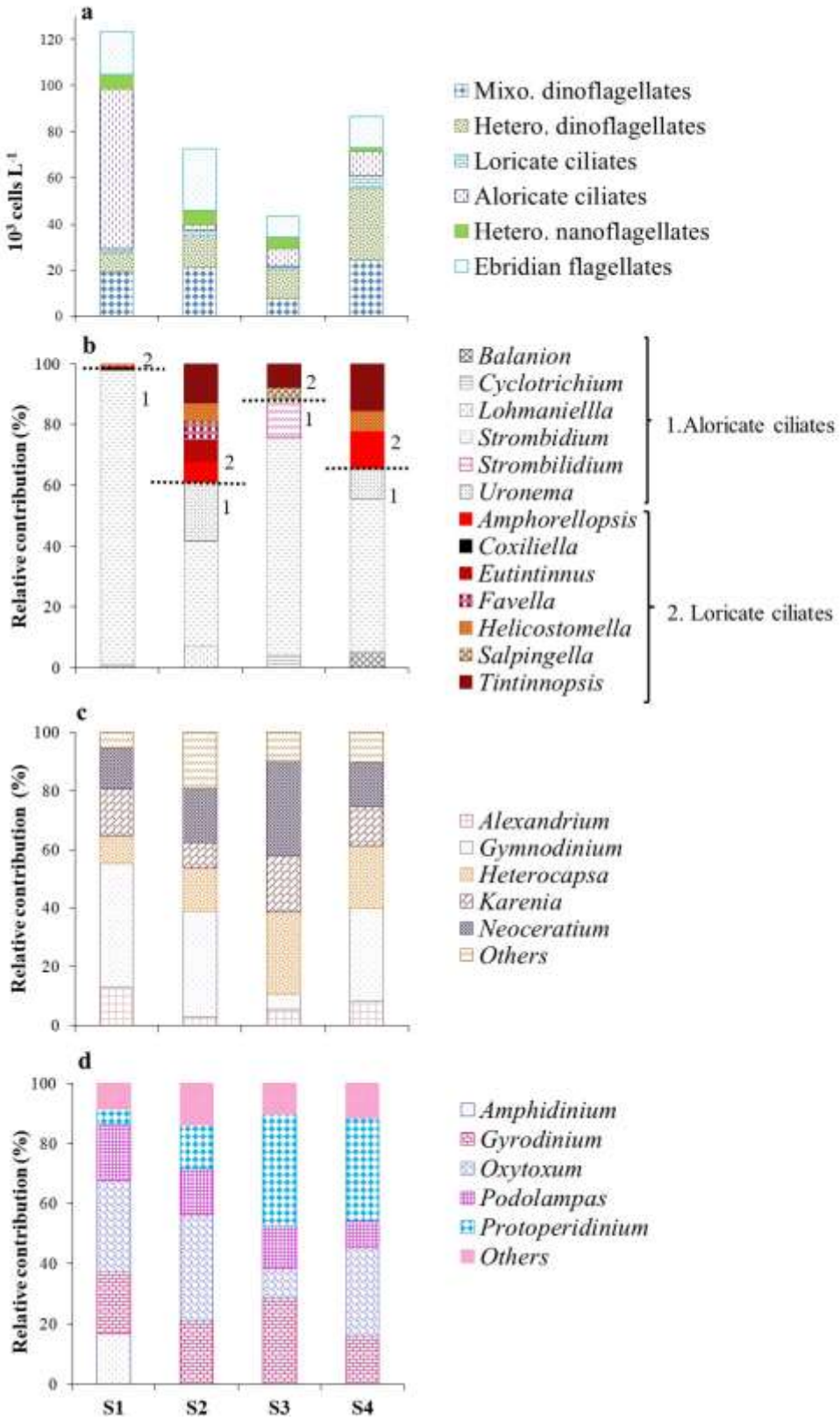

456

457 **Fig. 3** Abundance and composition of protozooplankton (**a**), and specific structure of the main
458 protozoan groups (**b-d**) in the sampling stations during the fall 2017. Values are the means of
459 the three depths at each station

Link: *https://link.springer.com/article/10.1007/s12601-023-00101-6*

Online ISSN 2005-7172
Print ISSN 1738-5261

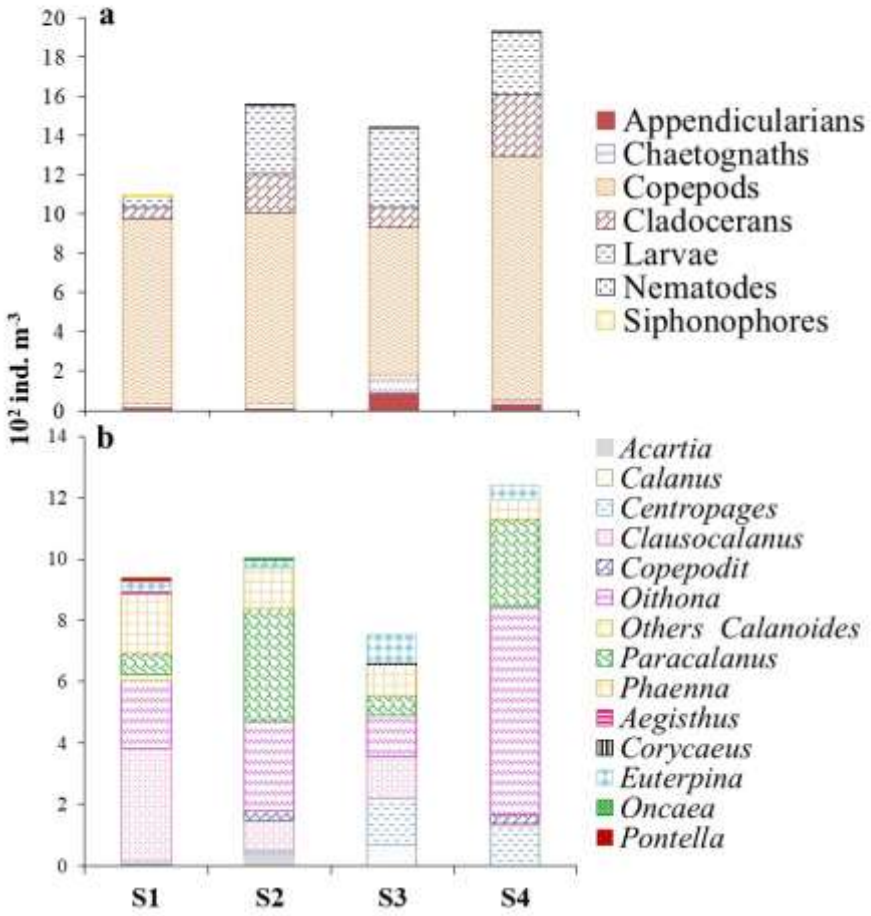

Fig. 4 Abundance and composition of metazooplankton groups (**a**), and copepod taxa (**b**) in the sampling stations during the fall 2017

Relationship between environmental conditions and plankton communities. The influence of physico-chemical factors on phytoplankton (the three size fractions) and zooplankton distribution, as well as relationships between phytoplankton and zooplankton were summarized by the CCA. The first two canonical components extracted 69% of the canonical variance (Fig. 5). A Monte Carlo permutation test showed that all canonical axes were highly significant ($p < 0.0001$). The positive pole of axis 1 was correlated with salinity (0.53, $p < 0.05$) and organic nitrogen (0.73, $p < 0.01$), while the negative pole was correlated with temperature (-0.51, $p < 0.05$), inorganic phosphorus (-0.61, $p < 0.05$), inorganic nitrogen (-0.50, $p < 0.05$),

Online ISSN 2005-7172
Print ISSN 1738-5261

silicates (-0.61, $p < 0.05$) and organic phosphorous (-0.65, $p < 0.05$). Axis 2 was positively correlated with the pH (0.53, $p < 0.05$).

The CCA discriminated two groups. The first axis positively selected picophytoplankton with abiotic variables such as salinity and organic nitrogen, while nano- and microphytoplankton were related to organic and inorganic phosphorus, silicates, inorganic nitrogen, and temperature. The CCA also showed that pico-sized cells were associated with aloricate ciliates, as well as heterotrophic and ebridian nanoflagellates. In contrast, nano- and microphytoplankton prevailed when dinoflagellates (mixo- and hetero-trophic organisms), loricate ciliates, copepods and cladocerans largely occurred. Dinoflagellates, loricate ciliates and copepods showed a positive correlation with temperature but were negatively correlated to salinity. Loricate ciliates and flagellates protozoans followed, however, the opposite trend.

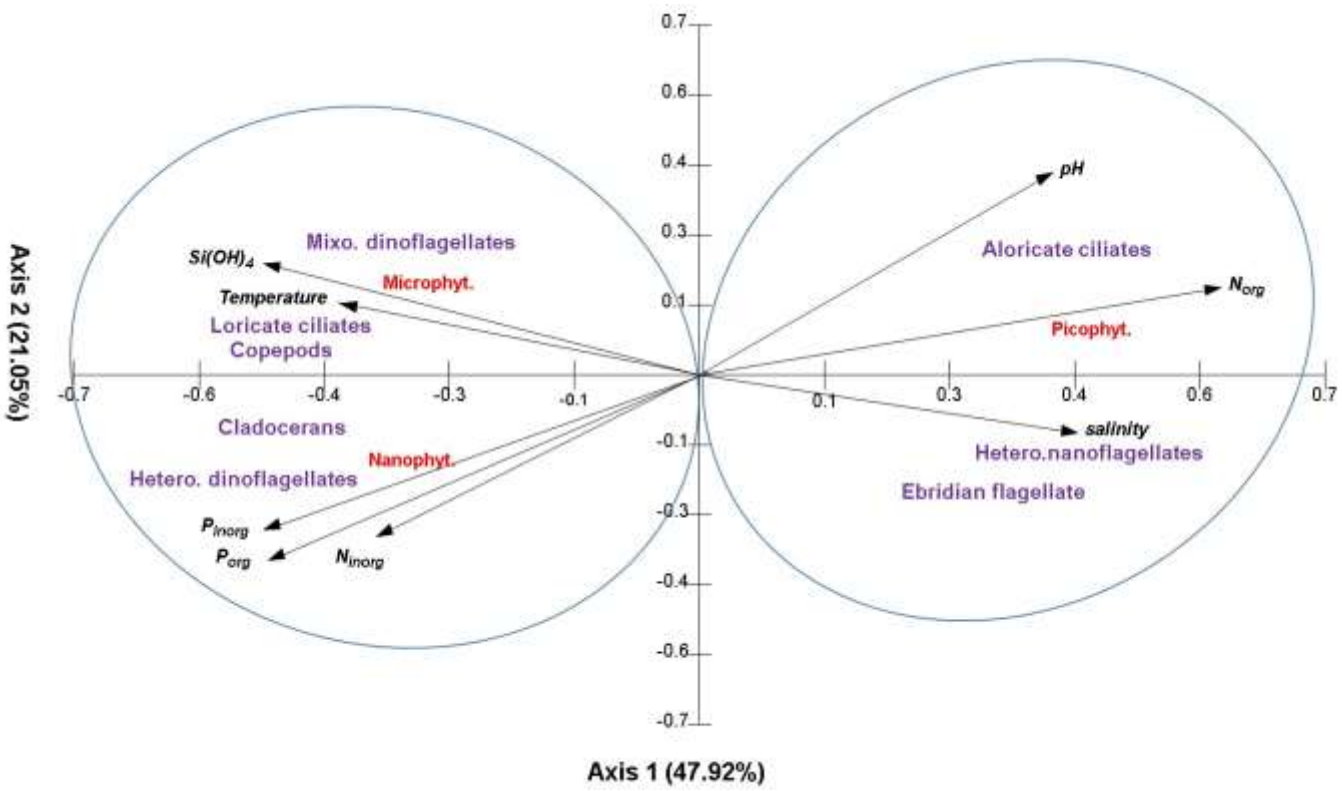

Fig. 5 Canonical correspondence analysis (CCA) ordination diagram showing the relationship between phytoplankton (the three size fractions), zooplankton, and physico-chemical factors

Online ISSN 2005-7172
Print ISSN 1738-5261

3.3. Phytoplankton growth and production

The growth rates varied significantly (ANOVA, $p < 0.01$) among stations and size fractions (micro-: 0.41-1.52 d^{-1}; nano-: 1.09-1.89 d^{-1}; pico-phytoplankton: 1.01-1.89 d^{-1}) (Fig. 6a). The highest rate for the pico-sized fraction was recorded in S1, whereas for nano- and micro-phytoplankton, the highest rates were observed in S4. The growth rate of microphytoplankton was positively correlated with inorganic N and P ($r_s = 0.73$-0.76, $p < 0.01$), while that of picophytoplankton showed negative correlations with these nutrients ($r_s = -0.62$ - 0.73, $p < 0.01$).

Production rates for size fractioned and total phytoplankton varied significantly among stations (ANOVA, $p < 0.05$; Fig. 6b). Picophytoplankton displayed a very high production rate in S1 (1412 mg C m^{-2} d^{-1}) in comparison to other stations (300-496 mg C m^{-2} d^{-1}). Microphytoplankton showed an opposite trend, with higher production rates in S2, S3 and S4 (1160-2075 mg C m^{-2} d^{-1}) than in S1 (188 mg C m^{-2} d^{-1}). The production rate for the micro-sized fraction was positively correlated to diatom biomass ($r_s = 0.83$, $p < 0.01$). Production rate for nanophytoplankton was low in S1 and S3 (188-215 mg C m^{-2} d^{-1}). Higher value was observed in S2 (452 mg C m^{-2} d^{-1}) and the highest in S4 (1301 mg C m^{-2} d^{-1}). Production rate for total phytoplankton showed an increasing trend from S1 (1816 mg C m^{-2} d^{-1}) to S4 (3873 mg C m^{-2} d^{-1}), and was positively correlated to all inorganic nutrients ($r_s = 0.68$-0.81, $p < 0.01$). In S2, S3 and S4, microphytoplankton was the main carbon producer (55-78%), whereas in S1 picophytoplankton provided 78% of total carbon production. Nanophytoplankton contributed only 7-12% of produced carbon in S1 and S3, and 21-34% in S2 and S4.

Online ISSN 2005-7172
Print ISSN 1738-5261

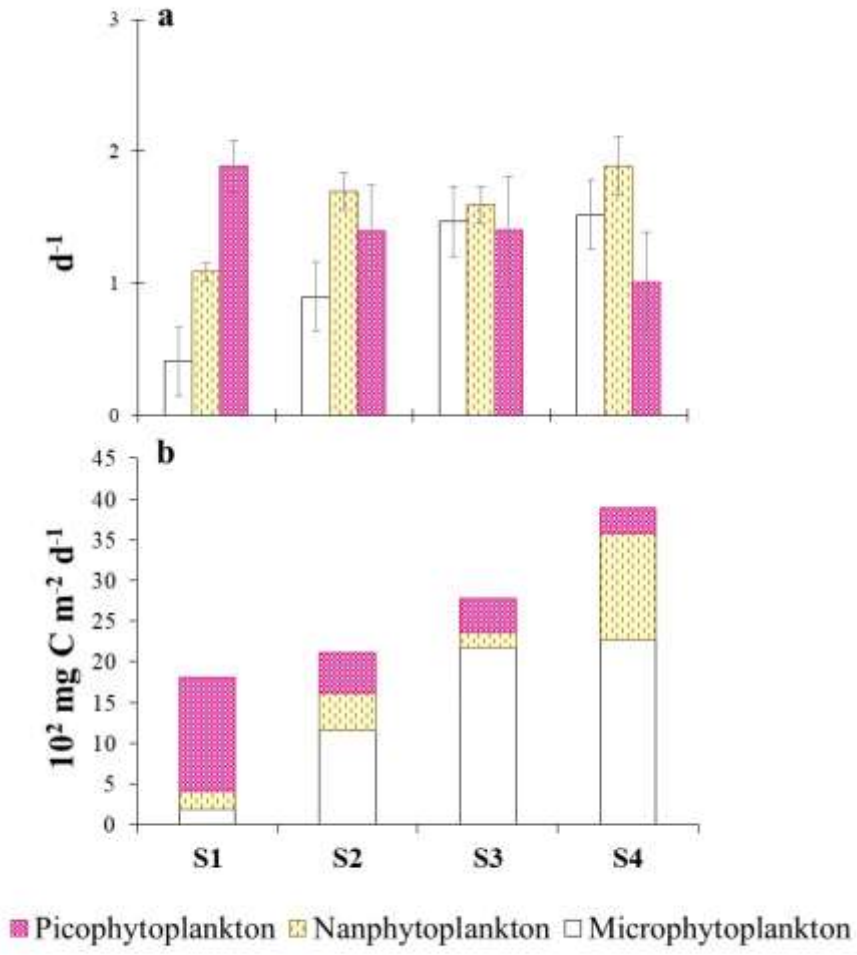

507

508 **Fig. 6** Growth (**a**) and production (**b**) rates of the three phytoplankton size fractions
509 (picophytoplankton: < 2 μm, nanophytoplankton: 2-10 μm, microphytoplankton: > 10
510 μm) in the sampling stations during the fall 2017

511 **3.4 Phytoplankton grazing**

512 **Grazing by protozooplankton**. The grazing and consumption rates by protozooplankton
513 varied significantly among size fractions and across stations (ANOVA, $p < 0.01$; Table 2).
514 Picophytoplankton was grazed at higher rates (0.82-1.30 d^{-1}) than the other size fractions
515 (micro-: 0.18-0.54 d^{-1}; nano-phytoplankton: 0.51-1.01 d^{-1}) in stations S1, S2 and S3. However,
516 microphytoplankton was the most grazed in S4 (0.84 d^{-1}). The highest consumption rate for
517 picophytoplankton was recorded in S1 (762.96 mg C m^{-2} d^{-1}) and the lowest in S4 (137 mg C

Online ISSN 2005-7172
Print ISSN 1738-5261

518 m^{-2} d^{-1}). In the opposite, nano- and micro-phytoplankton were consumed at low rates in S1
519 (92 and 71 mg C m^{-2} d^{-1}, respectively). Their consumption increased in other stations,
520 particularly in S4 (318 and 1049 mg C m^{-2} d^{-1}, respectively). For each size fraction, the
521 consumption rates showed positive correlations to the production rates (r_s = 0.73-0.95, $p < 0.05$).
522 The consumption rate for micro-sized fraction was positively correlated with the
523 abundances of heterotrophic dinoflagellates (r_s = 0.85, $p < 0.01$) and loricate ciliates (r_s = 0.60,
524 $p < 0.05$). Protozooplankton removed a substantial fraction of daily production for
525 picophytoplankton in most stations (~60% P grazed d^{-1}), except in S4 (40% P grazed d^{-1}). The
526 protozooplankton grazing corresponded to daily remove of 23-62% of nanophytoplankton
527 production. Protozooplankton grazing impact on microphytoplankton was higher in S4 (47%
528 P grazed d^{-1}) than in the other stations (22-41% P grazed d^{-1}). Furthermore, microbivory (carbon
529 from picophytoplankton) contributed to carbon ingestion of protozooplankton by only 9% in
530 S4, but by 24-34% in S2 and S3, and up to 82% in S1. Conversely, herbivory played a
531 significant role in the feeding of protozooplankton in the other stations, as microphytoplankton
532 alone represented 54-70% of their diet (Table 2).

533 **Grazing by metazooplankton.** The grazing rate and the impact of metazooplankton were
534 significantly different among stations (ANOVA, $p < 0.01$; Table 3). The consumption rate of
535 phytoplankton by metazooplankton showed the lowest value in S1 (76 mg C m^{-2} d^{-1}) and the
536 highest in S4 (794 mg C m^{-2} d^{-1}). This rate was positively correlated with nano- and
537 microphytoplankton biomass (r_s = 0.70-0.78, $p < 0.01$), and with copepod and cladoceran
538 abundances (r_s = 0.62-0.76, $p < 0.05$). Metazooplankton removed 10-24% of phytoplankton
539 production and 22-38% of phytoplankton standing stock (Table 3).

540

541

Online ISSN 2005-7172
Print ISSN 1738-5261

542 **Table 2** Grazing rates by protozooplankton (g), consumption rates of phytoplankton (G_p),
543 grazing impact on phytoplankton and protozooplankton diet in the sampling stations within the
544 Gulf of Gabès during the fall 2017 (Mean value ± SD, N = 3). p-value (ns: not significant; *:
545 0.01 < p < 0.05; ** 0.001 < p < 0.01, ***: p < 0.001) indicates the significant level for the
546 ANOVA used to test spatial variation.

547

	S1	S2	S3	*S4*	p-value
g (d^{-1})					
Microphyt.	0.18 ± 0.07	0.54 ± 0	0.38± 0.09	0.84 ± 0.03	***
Nanophyt.	0.88 ± 0.21	0.51 ± 0.15	0.71 ± 0.10	0.65 ± 0.21	*
Picophyt.	1.30 ± 0.04	0.88 ± 0.48	0.82 ± 0.80	0.68 ± 0.11	**
G_p (mg C m^{-2} d^{-1})					
Microphyt.	71.07 ± 17.46	463.79 ± 6.96	461.91 ± 103.73	1048.77 ± 48.25	**
Nanophyt.	91.74 ± 12.49	102.12 ± 29.80	119.45 ± 46.56	317.73 ± 16.81	*
Picophyt.	762.96 ± 6.35	293.91 ± 39.01	204.79 ± 30.00	137.50 ± 16.73	**
%P grazed d^{-1}					
Microphyt.	35 ± 15	40 ± 5	22 ± 4	47 ± 7	***
Nanophyt.	42 ± 5	23 ± 7	62 ± 20	40 ± 15	**
Picophyt.	60 ± 1	57 ± 6	56 ± 13	40 ± 4	**
Diet (%)					
Microphyt.	8 ± 3	54 ± 8	62 ± 7	70 ± 7	**
Nanophyt.	10 ± 3	12 ± 1	14 ± 8	21 ± 6	*
Picophyt.	82 ± 7	34 ± 7	24 ± 3	9 ± 1	*

548

549

550 **Table 3** Phytoplankton (nano- and micro-sized fractions) consumption rates by
551 metazooplankton and grazing impact in the sampling stations within the Gulf of Gabès during
552 the fall 2017. (Mean value ± SD, N = 3). p-value (ns: not significant; *: 0.01 < p < 0.05; **
553 0.001 < p < 0.01, ***: p < 0.001) indicates the significant level for the ANOVA used to test
554 spatial variation

	S1	S2	S3	S4	p-value
G_m (mg C m^{-2} d^{-1})	76.26 ± 0.65	313.36 ± 6.58	225.84 ± 2.40	794.28 ± 72.20	***
% P grazed d^{-1}	19 ± 1	20 ± 1	10 ± 5	24 ± 6	**
% Chl *a* grazed d^{-1}	22 ± 1	38 ± 3	32 ± 1	37 ± 4	ns

555

556

Online ISSN 2005-7172
Print ISSN 1738-5261

3.5 Vertical fluxes of particulate organic matter

The vertical fluxes of particles varied significantly among stations, from 561 mg C m^{-2} d^{-1} in S1 to 1891 mg C m^{-2} d^{-1} in S3 (ANOVA, $p < 0.05$; Fig. 7). These fluxes only accounted for 30% of primary production in S1, but reached 43-45% in S2 and S4, and 70% in S3. Detritus was the dominant sinking flux from S1 (78%) to S3 (79%), but contributed less to the vertical carbon flux of S4 (62%). The phytoplankton carbon exported towards the benthos followed an increasing trend from S1 (111 mg C m^{-2} d^{-1}) to S4 (611 mg C m^{-2} d^{-1}). Zooplankton fecal pellets were non-significant in S1, S2 and S3, and made only 2% of the vertical carbon flux in S4 (38 mg C m^{-2} d^{-1}).

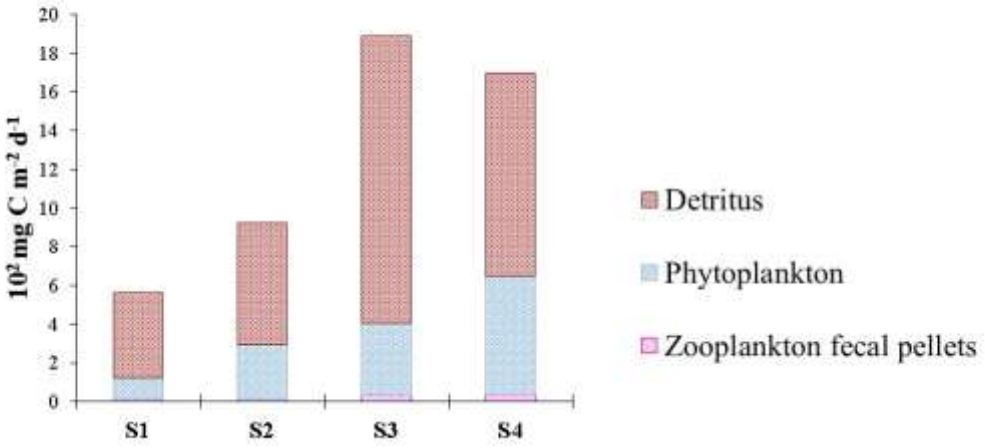

Fig. 7 Vertical fluxes of particulate organic carbon in the sampling stations during the fall 2017

3.6 Planktonic interactions

Based on data of size-fractionated production, prey-grazers relationships and carbon vertical flux, conceptual diagrams of planktonic interactions were established for all sampling stations (Fig. 8). The importance of the zooplankton microbivory and herbivory in the carbon transfer (i.e., total consumption by proto- and meta-zooplankton) were considered in each station.

Online ISSN 2005-7172
Print ISSN 1738-5261

In station S1, the primary production (1816 mg C m^{-2} d^{-1}) was lower than in the other stations, and mainly sustained by picophytoplankton (78%). These small producers were under strong grazing pressure by protozooplankton, which was dominated by aloricate ciliates. Consequently, a large amount of carbon (763 mg C m^{-2} d^{-1}) entered the food web *via* the microbivory of protozooplankton, which represented 76% of carbon transfer. However, > 2 µm phytoplankton (i.e., nano- and microphytoplankton), which was mainly composed by nano-sized phytoflagellates and to a lesser extent by diatoms, participated weakly to primary production (22%). Moreover, protozooplankton grazing on > 2 µm phytoplankton supplied small amounts of carbon to higher consumers (163 mg C m^{-2} d^{-1}). Metazooplankton had also low feeding on nano- and microphytoplankton (76 mg C m^{-2} d^{-1}). Consequently, herbivory of proto- and metazooplankton together represented only 24% of channeled carbon. Similar to primary production, the amount of carbon particles that settled down and could reach benthos was low (562 mg C m^{-2} d^{-1}).

In comparison to station S1, stations S2 and S3 had an increased production of > 2 µm phytoplankton, particularly of microphytoplankton forming more than 70% of the total primary production, simultaneously to an increase of the diatom abundance. This was accompanied by an increase in the herbivory of protozooplankton (48-60% of carbon transfer), which was dominated by mixotrophic and heterotrophic dinoflagellates and ebridian flagellates. Thus, a high amount of > 2 µm phytoplankton production (566-660 mg C m^{-2} d^{-1}) fueled the food web. Conversely, grazing impact of protozooplankton has decreased for picophytoplankton, which contributed moderately to primary production (15-24%), and hence protozooplankton microbivory (205-294 mg C m^{-2} d^{-1}) supplied 20-25% of carbon to food web. Herbivory of metazooplankton was relatively important (226-313 mg C m^{-2} d^{-1}), corresponding to 20-27% of carbon transfer. Similarly, vertical flux of particles increased in both stations to reach higher value (924-1891 mg C m^{-2} d^{-1}) than in S1.

Online ISSN 2005-7172
Print ISSN 1738-5261

In station S4, the production of picophytoplankton had further decreased, compared to other stations, to reach the lowest rate (8% of total PP) in detriment of an increase of the production of > 2 µm phytoplankton, which was characterized by the abundance of large diatoms (such as *Rhizosolenia setigera* and *Skeletonema costatum*). Therefore, herbivorous protozoans, such as the diatom-consumer *Protoperidinium*, were abundant, leading to increased herbivory for proto- (59%) and meta-zooplankton (35%), which supplied substantial quantities of carbon (1367 and 794 mg C m^{-2} d^{-1}, respectively) to food web. A significant carbon flux towards benthos was also observed in this station (1700 mg C m^{-2} d^{-1}).

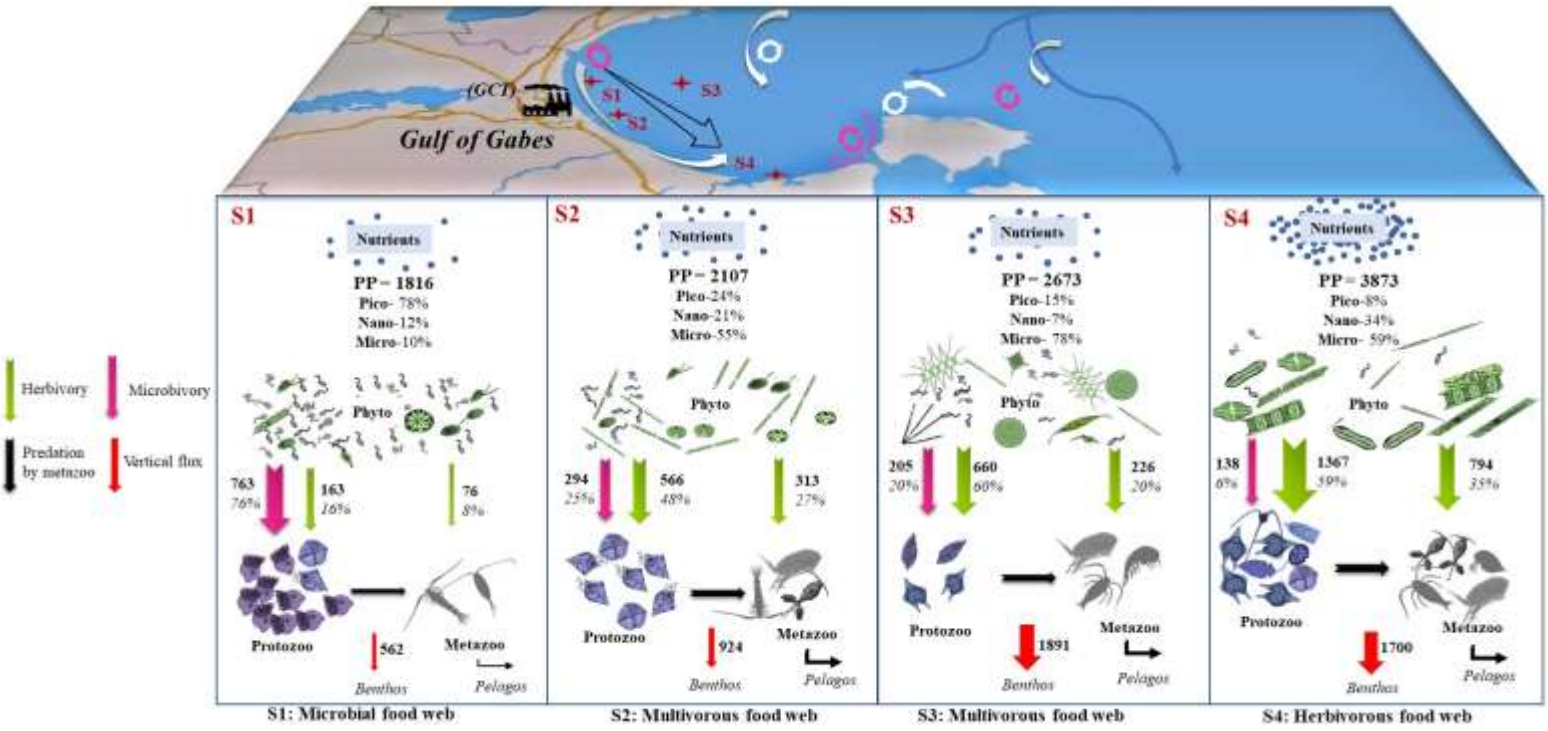

Fig. 8 Primary production (PP, mg C m^{-2} d^{-1}), trophic relationships and carbon transfer pathways within the planktonic systems of the sampling stations in link with the nutrient spatial gradient and hydrodynamic circulation in the Gulf of Gabès during the fall 2017. Percentage contributions of phytoplankton size fractions to PP are indicated. Values with arrows show the amount of channeled biogenic carbon (mg C m^{-2} d^{-1}) and percentages represent the contribution of zooplankton microbivory or herbivory to carbon transfer. Width of arrow is proportional to the carbon flow. Microbivory = consumption of Pico- by Protozoo; Herbivory = consumption of Nano- and Micro- by Protozoo and Metazoo; carbon transfer = consumption of Pico, Nano and Micro by Protozoo and Metazoo.

Online ISSN 2005-7172
Print ISSN 1738-5261

4 Discussion

4.1 Productivity and nutrient richness

Although the primary production levels are well documented for several Mediterranean regions (Psarra et al. 2005; Kovač et al. 2018), information remains scarce for the Southern Mediterranean (Sakka Hlaili et al. 2008; Meddeb et al. 2018) and even deficient for the GG. Here we provide primary production estimates in the GG based on dilution experiments. This technique has been already used in various marine systems, and has shown production rates that are similar to those measured by ^{14}C method (Moigis and Gocke 2003; Meddeb et al. 2018; Dokulil and Qian 2021). Nutrients were not added to dilution bottles, assuming high nutrient concentrations in the GG during our study period. The estimated growth rates were relatively high for most size fractions ($k \geq 1$ d^{-1}; Fig. 6a), indicating that nutrients were non-limiting for phytoplankton growth. Furthermore, our estimates of growth rates for different size fractions (0.4-1.9 d^{-1}) are in the range of values reported for fractioned phytoplankton from dilution experiments (with or without nutrient addition) in other coastal ecosystems (Grami et al. 2008; Wickham et al. 2022). Furthermore, Boudriga et al. (2022) recently reported similar growth rate (0.38-1.7 d^{-1}) for phtytoplankton to our study. Therefore, the growth coefficients and subsequently the calculated production rates measured in the present work are considered as realistic.

Previous observations have suggested that the high fish production of the GG was related to a high primary production (Halouani et al. 2016; Béjaoui et al. 2019). Our study reveals indeed high total phytoplankton production rates (130-370 mg C m^{-3} d^{-1} or 1816-3674 mg C m^{-2} d^{-1}), which were comparable with estimates from dilution technique in other coastal waters, including Mediterranean ecosystems (Moigis and Gocke 2003; Marquis et al. 2007; Grami et al. 2008). However, the primary production levels determined in the GG, located in the oligotrophic Eastern Mediterranean, far exceed rates currently reported for ecosystems within

Online ISSN 2005-7172
Print ISSN 1738-5261

the same basin, as Ionian Sea, Aegean Sea and Gulf of Trieste (Christaki et al. 2011; Šolić et al. 2010; Cibic et al. 2018). This suggests the influence of anthropogenic nutrient inputs, in addition to natural sources, in the GG leading to its high productivity. Our estimates of Chl *a* concentrations (1.65-6.06 µg L^{-1}) also surpassed values reported in Mediterranean open sea areas (Raveh et al. 2015; Salgado-Hernanz et al. 2019), but were in the range found in other coastal waters (Meddeb et al. 2018; Morsy et al. 2022). Our Chl *a* levels were higher than those recorded by previous studies in the offshore part of GG (< 1 µg L^{-1}; Bel Hassen et al. 2009; Hamdi et al. 2015), which can be due to several environmental features, such as hydrological conditions, nutrient content, season, and phytoplankton community composition. Most of previous works have been conducted during the summer-stratification period (July-September) or during the transition period from the mixed to the stratified water (May-June), when nutrients were in shortage (< 3 N µM, < 1 P µM) resulting in low Chl *a* concentrations. Furthermore, > 2 µm cells dominated the total Chl *a* in all stations (63-89%) and microphytoplankton alone formed ≥ 50% in S3 and S4 (Table 1). Moreover, large diatoms (*Leptocylindrus*, *Skeletonema* and *Rhizosolenia*) were dominant during our sampling period (Fig. 2a, b). All these observations may explain the higher Chl *a* concentrations measured during our study compared to previous works, which reported the dominance of pico- and nano-sized phototrophs and the scarcity of diatoms (Bel Hassen et al. 2009; Hamdi et al. 2015; Khammeri et al. 2020).

The high primary production and Chl *a* concentrations in the GG were associated to high nutrient concentrations (Table 1), mainly due to the large supply from anthropogenic discharges and also to tide-induced sediment resuspension and atmospheric deposition (Drira et al. 2016; Khammeri et al. 2018). The GG is exceptionally enriched in inorganic and organic P (Table 1) since it continuously receives large amounts of phosphogypsum (1,000 to 13,000 t *per* day since the 1970's) from the phosphoric acid plant (Béjaoui et al. 2004; Khedhri et al. 2014). The P_{inorg} concentrations measured in all stations exceed those usually observed in Mediterranean coastal waters, like the lagoons of Bizerte (0.15 µM; Meddeb et al. 2018) and Thau (0.18 µM;

Online ISSN 2005-7172
Print ISSN 1738-5261

Courboulès et al. 2021), and the Gulf of Lion (0.06-0.12 µM; Ross et al. 2016). The continuous nutrient enrichment caused by anthropogenic inputs could lead to enhanced eutrophication of the GG, causing ecosystem imbalance in the future. Signs of eutrophication, such as occurrence of harmful algal blooms, have indeed been often reported (Feki- Sahnoun et al. 2017; Ayata et al. 2018).

In the GG, a North-South and coast-offshore gradient of nutrients (Fig. S1) and organic matter with accumulation in the Southern part has been already observed (Ciglenečki et al. 2020; Mansouri et al. 2020). This spatial pattern can be related to the hydrodynamics of the GG, which is characterized by the presence of a stationary southward current, two great eddies in the middle, and a counter current in the Southern part (Fig. 1; Zayen et al. 2020). During our study, nutrients also showed increasing concentrations from the North (S1) to the South (S4) and from the coast (S1) to offshore (S3). Phytoplankton variables (i.e., production, carbon biomass and Chl *a*) followed the same spatial distribution patterns than nutrients, confirming that spatial distribution of Chl *a* is closely related to nutrient concentrations in the GG (Bel Hassen et al. 2009).

4.2 Spatial dynamics of phytoplankton

There was a clear spatial variability in the size structure of phytoplankton. The dominance of fast-growing picophytoplankton in S1 (Table 1, Fig. 6a, b) confirmed its main functional role in this station. In general, the picophytoplankton is dominant in oligotrophic Mediterranean open sea, such as the Northern Adriatic Sea, the Levantine Basin, the Southern Tyrrhenian Sea and the Southern Adriatic Sea (Totti et al. 2005; Tanaka et al. 2007; Decembrini et al. 2009; Cerino et al. 2012). Our results reveal that picophytoplankton can be an important component within the phytoplankton community in coastal Mediterranean waters, with relatively important nutrient concentrations (i.e., in S1). Unlike S1, large phytoplankton characterized the other stations, even the offshore station (i.e., S3). The micro-sized fraction contributed most of the

Online ISSN 2005-7172
Print ISSN 1738-5261

primary production (55-78%) and carbon biomass (71-75%) in S2, S3 and S4, and dominated the Chl *a* (49-74%) in S3 and S4 (Table 1, Fig. 6b). The nutrient spatial gradient induced by hydrodynamic features has likely influenced the spatial distribution of phytoplankton size fractions. This was evidenced by a positive correlation between the growth rate of micro-sized fraction and inorganic nutrients, and a negative correlation for the pico-fraction growth rate. The CCA showed also that large phytoplankton was associated with all inorganic nutrients while an opposite trend was found for the picophytoplankton (Fig. 5). Jyothibabu et al. (2015) have reported a clear impact of the hydrodynamics (summer monsoon current and associated eddies) on the evolution of nutrients and phytoplankton size structure in the Bay of Bengal (Northeastern Indian Ocean). Recently, Decembrini et al. (2020) have showed that the circulation within the Gulf of Augusta (Western Ionian Sea) allowed the advection of nutrient-rich waters that modified the size structure of phytoplankton and triggered an increase of the micro-sized fraction.

The > 2 µm phytoplankton community also displayed a spatial variation in species composition. Generally, nano-sized phytoflagellates, mainly represented by cryptophyceae, dominated in biomass in S1, typified by the least rich waters of the majority of nutrients (lowest concentrations of P_{inorg}, $P_{org,}$ and $Si(OH)_4$). Conversely, the contribution of diatoms increased from S1 (37%) to S4 (88%) concomitantly with the nutrient increase. Diatom biomass showed a positive correlation with all inorganic nutrients (r_s = 0.79-0.67, $p < 0.01$). It is well known that small phototrophs with high surface-to-volume ratio require lower nutrient concentrations for their growth than large cells, which grow well under more nutrient enriched waters (Duarte et al. 2000; Varkitzi et al. 2020). This may explain the high contribution of nano-sized cells to the > 2 µm phytoplankton community and the dominance of picophytoplankton in S1. The high contribution of nano-sized cells, such as chlorophyceae, cryptophyceae and prymnesiophyceae, to phytoplankton community was previously reported in the GG during a period characterized by reduced nutrient supply (Bel Hassen et al. 2009; Ben Ltaief et al. 2015; Rekik et al. 2015).

Online ISSN 2005-7172
Print ISSN 1738-5261

Nano-sized phytoflagellates are typical of waters with low nutrient concentrations, such as Mediterranean open sea areas (Vidussi et al. 2000; Decembrini et al. 2009). In contrast, blooms of diatoms are commonly observed in coastal Mediterranean environments, particularly during late winter-spring (d'Alcalà et al. 2004; Mayot et al. 2017; Leblanc et al. 2018), when the stratification of the water column follows the vertical mixing, thus favoring the growth of small species (such as *Chaetoceros*) (Peters et al. 2006; Trombetta et al. 2021). Other authors have rather reported the presence of diatoms in Mediterranean waters during the period of turbulence (i.e., autumn), with high proliferation of large species (Margalef 1978; Decembrini et al. 2009; Vascotto et al. 2021). This agrees with our finding showing that micro-sized diatoms (*Leptocylindrus*, *Skeletonema* and *Rhizosolenia*) were dominant during our study period.

The decrease of picophytoplankton contribution to total primary production and Chl *a* content from S1 to S4, and the increase of micro-sized contribution and diatom proliferation would greatly influence the size and the type of grazers, as well as their feeding activity, suggesting a significant change in carbon transfer pathways between stations. These effects are detailed in the following sections.

4.3 Spatial variation of top-down control by metazooplankton

Copepods were dominant in the GG (Fig. 4a), as previously observed in this area (Drira et al. 2017; Makhlouf Belkahia et al. 2021) and in other Mediterranean ecosystems (Sakka Hlaili et al. 2008; Ben Lamine et al. 2015; Gueroun et al. 2020). The abundance of copepods found here (0.939-1240 × 10^3 ind m^{-3}) compared also well with previous reports in the GG (Ben Ltaief et al. 2017; Drira et al. 2017) and in other Mediterranean systems, i.e., Lagoons of Bizerte, Venice and Berre (Riccardi 2010; Siokou-Frangou et al. 2010; Marques et al. 2015; Gueroun et al. 2020). Our study assessed the feeding impact of metazooplankton on phytoplankton using the gut fluorescence method. This simple technique has been widely used for more than several decades because it is useful for revealing the functional role of

Online ISSN 2005-7172
Print ISSN 1738-5261

metazooplankton in various marine environments (Tseng et al. 2008; Meddeb et al. 2018; He et al. 2021). The results show that metazooplankton had an important control on phytoplankton, by consuming 10-24% of the primary production. This feeding effect exceeded that reported in other world oceanic regions (12%, Calbet et al. 2000), but compared with estimates from the gut fluorescence method in other Mediterranean ecosystems (8-30% P grazed d^{-1} in the Lagoon of Bizerte and 9-20% P grazed d^{-1} in the Alboran Sea) (Gaudy et al. 2003; Meddeb et al. 2018). The impact of metazooplankton on phytoplankton biomass (22-38% Chl *a* d^{-1}) was also in the range of percentages found by other authors (using the gut content technique) in coastal ecosystems, such as Gironde estuary, and Gulf of Mexico (Sautour et al. 2000; Landry and Swalethorp 2021). The significant percentages of phytoplankton biomass and production daily consumed by metazooplankton suggested the importance of the metazoan grazers in channeling carbon to higher trophic level in the GG.

The consumption by metazooplankton varied significantly among stations (Table 3), in relation with spatial variations of metazoan abundance (r_s = 0.62-0.76, $p < 0.05$) and prey biomass (r_s = 0.70-0.78, $p < 0.01$). Besides, change in size structure of phytoplankton seemed to influence the feeding of metazooplankton. Consumption rates of phytoplankton measured from S2 to S4 were 3-10 folds higher than that in S1, where the phytoplankton production was dominated by the pico-sized fraction, which is inefficiently consumed by copepods (Berggreen et al. 1988; Morales et al. 1993; Callieri and Stockner 2002). Conversely, the highest feeding activity of metazooplankton was observed in the southernmost station (S4), where large phytoplankton dominated the Chl *a* and primary production (Table 1, Fig. 6b). This coincided with a high proliferation of herbivorous copepods (e.g., *Centropages*, *Clausocalanus* and *Paracalanus*) and herbivorous cladocerans (e.g., *Penilia*, Katechakis et al. 2004) (Fig. 4a). The CCA also showed a clear association between the two metazoan groups and nano- and microphytoplankton (Fig. 5), which might be due to trophic relationships. As explained, the complex circulation in the GG favoured the accumulation of particles towards the South –

Online ISSN 2005-7172
Print ISSN 1738-5261

among which zooplankton and phytoplankton – leading to increased trophic interactions between the two planktonic components. Similarly, a recent work highlighted the role of hydrodynamics in the retention of metazooplankton in the Southern area of the GG and in the enhancement of its potential control of phytoplankton (Makhlouf Belkahia et al. 2021).

4.4 Spatial variation of top-down control by protozooplankton

Our study examined the impact of protozooplankton grazing on phytoplankton using the standard dilution method. This simple technique, which gives simultaneous estimations of growth and grazing rates, has been used over the past decades in open and coastal environments, including Mediterranean systems (Calbet and Landry 2004; Calbet et al. 2008; Grinienė et al. 2016; Leruste et al. 2019; Pecqueur et al. 2022; Wickham et al. 2022). However, the dilution method has been employed to a lesser extend for the estimation of protozooplankton grazing in the Southern Mediterranean (Sakka Hlaili et al. 2008; Grami et al. 2008; Meddeb et al. 2018). Furthermore, the functional role of protozooplankton is poorly documented in the GG, although previous studies have reported high abundances of ciliates, heterotrophic and mixotrophic flagellates (Hannachi et al. 2008; Drira et al. 2008; Kchaou et al. 2009; Hamdi et al. 2015; Ben Ltaief et al. 2017; Rekik et al. 2021).

Different size fractions of phytoplankton were measured in our dilution bottles rather than total phytoplankton in order to give an insight into the size-selective protozooplankton feeding. The dilution experiments provided statistically significant grazing estimates for different phytoplankton size fractions in all stations (Fig. S2 in Supplementary Material). Grazing rates may be over-estimated, if nutrient limitation occurs during experiment (Landry and Hassett 1982). In our work, although nutrients were not added, the phytoplankton growth was kept under unlimited conditions. Moreover, our estimates of grazing rates for pico-sized fraction were in the range of values reported from dilution experiments (with or without nutrients) in other coastal waters (Dong et al. 2021; Pecqueur et al. 2022). Using the same method, several

Online ISSN 2005-7172
Print ISSN 1738-5261

798 authors have also found grazing rates for nano- and microphytoplankton (Sakka Hlaili et al.
799 2007; Dong et al. 2021) comparable to our estimates (Table 2).

800 In general, there is a close and a positive trophic interaction between the growth of prey
801 and their grazing by protozooplankton (Shinada et al. 2000; Martin-Cereceda et al. 2003;
802 Dopheide et al. 2011; Chen et al. 2020). Indeed, for each size-fraction, significant and positive
803 correlations were found between prey production and protozooplankton consumption rates.
804 Several studies have shown that protozoan organisms were able to modify their growth
805 according to the availability of their potential prey and that the change in phytoplankton size
806 structure may influence the community composition of protozooplankton and its grazing
807 pressure (Sherr and Sherr 2007; Mansano et al. 2014; Horn et al. 2020; Corradino and Schnetzer
808 2022; Li et al. 2022). The high proliferation of picophytoplankton in S1 was associated with a
809 clear dominance of small aloricate ciliates (20-50 µm *Strombidium* spp.; Fig. 3a), which are
810 known to have large predation on pico-sized cells (Rassoulzadegan et al. 1988; Sakka 2000;
811 Meddeb et al. 2018). Heterotrophic nanoflagellates (*Commotion cryoporinum*) and ebridian
812 flagellates (*Hermesinium sp.*), which can actively consume pico-sized prey (Hargraves 2002;
813 Calbet and Landry 2004; Berglund et al. 2007), were well represented in S1 (Fig. 3a). The CCA
814 analysis showed likewise a strong association, likely through feeding links, between
815 picophytoplankton biomass and the abundances of all these microbivorous consumers (Fig. 5).
816 Accordingly, the protozooplankton displayed high consumption rate and grazing impact on the
817 pico-sized fraction in S1 (60% P grazed d^{-1}), testified by the large contribution of the
818 picophytoplankton to the protozoan diet (82%) (Table 2). Our result is consistent with the
819 finding of high grazing pressure of protozooplankton on picophytoplankton in other
820 Mediterranean coastal systems, such as the Bizerte Channel (84% P grazed d^{-1}) and Thau
821 Lagoon (71% P grazed d^{-1}) (Bec et al. 2005; Meddeb et al. 2018). Grazing and consumption
822 rates for the pico-sized fraction showed a decreased trend from S1 to S4, where the
823 protozooplankton community has clearly changed towards a dominance of heterotrophic and

Online ISSN 2005-7172
Print ISSN 1738-5261

mixotrophic dinoflagellates (Fig. 3a), concomitantly to the increase of large phytoplankton proliferation (Table 1, Fig. 6). In S4, heterotrophic dinoflagellates were dominated by species of *Protoperidinum* and *Oxytoxym* (Fig. 3d), which are known as potential grazers of chain-forming diatoms and small diatoms, respectively (Seong et al. 2006; Girault et al. 2013; Kase et al. 2021). Mixotrophic dinoflagellates were dominated by *Heterocapsa* and *Gymnodinium* (Fig. 3c) that can feed on small diatoms and nano-sized cells (Du Yoo et al. 2009; Jeong et al. 2010). The loricate ciliates, mainly *Tintinnopsis*, *Helicostomella* and *Amphorellopsis*, which commonly feed on large algae (Dolan et al. 2012; Yang et al. 2019), were more abundant in S4 than in other stations (Fig. 3a). All these herbivorous protozoans seemed to be tightly associated, probably *via* feeding links, to nano- and micro-phytoplankton (CCA analysis, Fig. 5). Thus, the highest consumption rates for nano- and micro-sized fractions were recorded in S4. In this station, the protozoan's diet mainly relied on microphytoplankton (70%), which accordingly was under the greatest protozooplankton grazing effect (~50% P grazed d^{-1}) (Table 2). In S4, although metazoans displayed increased abundance and very high consumption rates (Table 3; Fig. 4), their grazing impact (24% P grazed d^{-1}) remained lower than that of protozooplankton, which daily consumed 48% of the > 2-µm phytoplankton production. Our finding is in good agreement with several authors stating that protozooplankton is the major grazer of phytoplankton in productive waters dominated by large phytoplankton (Aberle et al. 2007; Vargas et al. 2007; Meddeb et al. 2018; Yang et al. 2022). In S2 and S3, nano- and micro-sized fractions formed large proportions of phytoplankton production and biomass (Chl *a* and carbon). The contribution of picophytoplankton was not as low, reaching ~20% of biomass and production of phytoplankton (Table 1; Fig. 6a). Accordingly, microbivorous protozoans (i.e., aloricate ciliates, heterotrophic nanoflagellates and ebridian flagellates) and herbivorous organisms (i.e., dinoflagellates) were both important components of the protozooplankton in both stations (Fig. 3). This resulted in significant protozooplankton top-down control on large and small phytoplankton in S2 and S3 (Table 2).

Online ISSN 2005-7172
Print ISSN 1738-5261

4.5 Implication for carbon transfer pathway

Anthropogenic nutrient inputs coupled with a complex hydrodynamic circulation in the GG led to a clear spatial gradient in nutrients, associated with spatial changes in composition and size structure of phytoplankton and selective zooplankton grazing. Microbivory and herbivory would therefore have different roles in carbon transfer (Fig. 8), inducing different trophic structures among stations.

In the northernmost station (S1), characterized by less nutrient-rich waters, the high contribution of picophytoplankton (78%) to the primary production was associated with a high microbivory of protozooplankton, representing 76% of carbon transfer. Therefore, the feeding of the microbivorous protozoans played the main role in carbon transfer to upper consumers (76%), as the herbivory of proto- and meta-zooplankton contributed together only 24% of the channeled carbon. These trophic interactions suggest the prevalence of the microbial food web in S1 (Legendre and Rassoulzadegan 1995; Sakka Hlaili et al. 2014), which is different from the traditional view regarding the presence of the microbial pathway in oligotrophic waters. Nevertheless, there is increasing evidence that microbial food web can be significant for eutrophic coastal areas (Grami et al. 2008; Viñas et al. 2013; Paklar et al. 2020). The situation has changed in S2 and S3, evidenced by the increased contribution of microphytoplankton to primary production (55-78%), albeit the pico-sized cells remained as substantial contributor to carbon production (15-24%). Parallel to the increase of large phytoplankton production, the herbivory of proto- and metazooplankton increased, forming 75-80% of biogenic carbon channeling. The consumption of picophytoplankton allowed 20-25% transfer of biogenic carbon. Therefore, pico-, nano- and micro-phytoplankton potentially contributed to the production of biogenic carbon, which reached higher consumers through the microbivory and the herbivory of zooplankton. This suggests that a multivorous food web (Legendre and Rassoulzadegan 1995) was present in both stations. The multivorous pathway was already

Online ISSN 2005-7172
Print ISSN 1738-5261

observed in other productive waters (Vargas and González 2004; Siokou-Frangou et al. 2010; Masclaux et al. 2015; Meddeb et al. 2018). In the southernmost nutrient-rich station (S4), the herbivorous food web seemed to be dominant, since the high primary production was mainly sustained by microphytoplankton (~60%) and the biogenic carbon was mainly channeled to higher trophic levels through the proto- and meta-zooplankton herbivory, which represented 94% of total carbon transfer. The herbivorous pathway was reported in several coastal waters with high trophic level and abundant diatoms (Sakka Hlaili et al. 2008; Masclaux et al. 2015; Meddeb et al. 2018; D'Alelio et al. 2022). The co-existence of different and contrasted planktonic food webs during the same period in a highly productive system (i.e., the GG) diverges from the traditional view that large phytoplankton and herbivorous pathway usually dominate in nutrient-rich waters.

The spatial variability in planktonic food webs has an ecological implication, as biogenic carbon can be exported with different efficiency to pelagos and benthos (Legendre and Rassoulzadegan 1995; Sakka Hlaili et al. 2014). The microbial food web is known to be inefficient in exporting organic matter, as most of the carbon is recycled and a small amount of carbon can be exported to higher consumers or outside euphotic system (Legendre and Rassoulzadegan 1995; Decembrini et al. 2009). This was consistent with the low vertical carbon flux found in S1, which only accounted for 30% of total primary production. In the other stations, the increase of primary production and of the dominance of large phytoplankton was associated with the increase of vertical flux of organic particles (43-70% of primary production). Furthermore, phytoplankton and zooplankton fecal material showed increased contribution to the carbon flux toward the benthos (Fig. 7). This confirms that more biogenic carbon is exported towards multivorous and herbivorous food webs (Legendre and Rassoulzadegan 1995; Meddeb et al. 2019). The highest phytoplankton export to benthos was observed in S4, coinciding with the largest contribution of microphytoplankton to primary

Online ISSN 2005-7172
Print ISSN 1738-5261

production. Conversely, the highest detritus sinking flux was not measured in S4 but in S3. This indicates that some of the sinking detrital material in S3 could be transported from elsewhere.

The hydrodynamic and hydrological features of this area change across seasons, which can impact the plankton dynamics (Bel Hassen et al. 2008, 2009; Makhlouf Belkahia et al. 2021) as well as planktonic interactions within the ecosystem. Thus, it is important to consider the seasonal variations in further investigations to better understand the overall functioning of this high dynamical and productive Mediterranean area.

5 Conclusion

Our study provides a detailed analysis of the plankton communities and the trophic links between size fractionated phytoplankton and proto/metazooplankton in a nutrient-rich and highly productive Mediterranean system, the GG. The complex hydrodynamic circulation within the GG seemed to induce a spatial gradient in nutrient concentrations driving a spatial changes in size structure and production of phytoplankton and trophic interactions, ultimately leading to various food webs structure with different efficiency in carbon export. Our results allows changing our traditional view concerning the dominance of the herbivorous pathway in highly productive areas and evidencing the presence of a trophic pathway continuum, with other types of planktonic food webs. Our study gives relevant insight on the functional roles of phytoplankton size fractions, proto- and meta-zooplankton and proposes a first description of carbon transfer pathways in the Southeastern Mediterranean area, where such information is deficient. These results can improve the understanding of the dynamics of marine food webs, particularly in ecosystems strongly impacted by anthropogenic nutrient inputs and strong hydrodynamics.

Online ISSN 2005-7172
Print ISSN 1738-5261

References

Abdennadher J, Boukthir M (2006) Numerical simulation of the barotropic tides in the Tunisian Shelf and the Strait of Sicily. J Mar Syst 63:162–182. https://doi.org/10.1016/j.jmarsys.2006.07.001

Aberle N, Lengfellner K, Sommer U (2007) Spring bloom succession, grazing impact and herbivore selectivity of ciliate communities in response to winter warming. Oecologia 150:668–681. https://doi.org/10.1007/s00442-006-0540-y

Allen JI, Somerfield PJ, Siddorn J (2002) Primary and bacterial production in the Mediterranean Sea: a modelling study. J Mar Syst 33–34:473–495. https://doi.org/10.1016/S0924-7963(02)00072-6

Ayata S-D, Irisson J-O, Aubert A, Berline L, Dutay JC, Mayot N, Nieblas AE, D'Ortenzio F, Palmiéri J, Reygondeau G, Rossi V, Guieu C (2018) Regionalisation of the Mediterranean basin, a MERMEX synthesis. Progress in Oceanography 163:7–20. https://doi.org/10.1016/j.pocean.2017.09.016

Bec B, Ratréma Husseini J, Collos Y, Souchu P, Vaquer A (2005) Phytoplankton seasonal dynamics in a Mediterranean coastal lagoon: Emphasis on the picoeukaryote community. J Plankton Res 0142-7873 Oxf Univ Press 2005-09 Vol 27 N 9 P 881-894 27:. https://doi.org/10.1093/plankt/fbi061

Béjaoui B, Ben Ismail S, Othmani A, Ben Abdallah-Ben Hadj Hamida O, Chevalier C, Feki-Sahnoun W, Harzallah A, Ben Hadj Hamida N, Bouaziz R, Dahech S, Diaz F, Tounsi K, Sammari C, Pagano M, Bel Hassen M (2019) Synthesis review of the Gulf of Gabes (eastern Mediterranean Sea, Tunisia): Morphological, climatic, physical oceanographic, biogeochemical and fisheries features. Estuar Coast Shelf Sci 219:395–408. https://doi.org/10.1016/j.ecss.2019.01.006

Béjaoui B, Raïs S, Koutitonsky V (2004) Modélisation de la dispersion du phosphogypse dans le golfe de Gabès. Modelisation of the phosphogypsum spreading in the gulf of Gabes. Bull. Inst. Natn. Scien. Tech. Mer de Salammbô, Vol. 31.

Bel Hassen M, Drira Z, Hamza A, Ayadi H, Akrout F, Issaoui H (2008) Summer phytoplankton pigments and community composition related to water mass properties in the Gulf of Gabes. Estuar Coast Shelf Sci 77:645–656. https://doi.org/10.1016/j.ecss.2007.10.027

Bel Hassen M, Hamza A, Drira Z, Zouari A, Akrout F, Messaoudi S, Aleya L, Ayadi H (2009) Phytoplankton-pigment signatures and their relationship to spring–summer stratification in the Gulf of Gabes. Estuar Coast Shelf Sci 83:296–306. https://doi.org/10.1016/j.ecss.2009.04.002

Ben Ismail S, Sammari C, Pietro Gasparini G, Beranger K, Brahim M, Aleya L (2012) Water masses exchanged through the Channel of Sicily: Evidence for the presence of new water masses on the Tunisian side of the channel. Deep Sea Research Part I: Oceanographic Research Papers Vol 63, May 2012, Pages 65-81. https://doi.org/10.1016/j.dsr.2011.12.009

Online ISSN 2005-7172
Print ISSN 1738-5261

963 Ben Ismail S, Sammari C, Béranger K (2015) Surface Circulation Features along the Tunisian
964 Coast: Central Mediterranean Sea. 26th IUGG General Assembly, Prague. Czech
965 Republic June 22 – July 2.

966 Ben Lamine Y, Pringault O, Aissi M, Ensibi C, Mahmoudi E, Kefi O D Y, Yahia M N D (2015)
967 Environmental controlling factors of copepod communities in the Gulf of Tunis (south
968 western Mediterranean Sea). Cah Biol Mar 56:213–229.

969 Ben Ltaief T, Drira Z, Devenon J L, Hamza A, Ayadi H, Pagano M (2017) How could thermal
970 stratification affect horizontal distribution of depth-integrated metazooplankton
971 communities in the Gulf of Gabes (Tunisia)?. Mar. Biol. Res. 13: 3.
972 https://www.tandfonline.com/doi/abs/10.1080/17451000.2016.1248847

973 Ben Ltaief T, Drira Z, Hannachi I, Bel Hassen M, Hamza A, Pagano M, Ayadi H (2015) What
974 are the factors leading to the success of small planktonic copepods in the Gulf of Gabes,
975 Tunisia? J Mar Biol Assoc U K 95:747–761.
976 https://doi.org/10.1017/S0025315414001507

977 Berglund J, Müren U, Båmstedt U, Andersson A (2007) Efficiency of a phytoplankton-based
978 and a bacterial-based food web in a pelagic marine system. Limnol Oceanogr 52:121–
979 131. https://doi.org/10.4319/lo.2007.52.1.0121

980 Berggreen U, Hansen B, Kiørboe T (1988) Food size spectra, ingestion and growth of the
981 copepodAcartia tonsa during development: Implications for determination of copepod
982 production. Mar Biol 99:341–352. https://doi.org/10.1007/BF02112126

983 Boudriga I, Thyssen M, Zouari A, Garcia N, Tedetti M, Bel Hassen M (2022)
984 Ultraphytoplankton community structure in subsurface waters along a North-South
985 Mediterranean transect. Marine Pollution Bulletin 182:113977.
986 https://doi.org/10.1016/j.marpolbul.2022.113977

987 Boukthir M, Jaber IB, Chevalier C, Abdennadher J (2019) A high-resolution three-dimensional
988 hydrodynamic model of the gulf of Gabes (Tunisia). In 42nd CIESM Congress.

989 Boutrup PV, Moestrup Ø, Tillmann U, Daugbjerg N (2016) Katodinium glaucum
990 (Dinophyceae) revisited: proposal of new genus, family and order based on
991 ultrastructure and phylogeny. Phycologia 55:147–164. https://doi.org/10.2216/15-138.1

992 Calbet A, Landry MR (2004) Phytoplankton growth, microzooplankton grazing, and carbon
993 cycling in marine systems. Limnol Oceanogr 49:51–57.
994 https://doi.org/10.4319/lo.2004.49.1.0051

995 Calbet A, Landry MR, Scheinberg RD (2000) Copepod grazing in a subtropical bay: species-
996 specific responses to a midsummer increase in nanoplankton standing stock. Mar Ecol
997 Prog Ser 193:75–84. https://doi.org/10.3354/meps193075

998 Calbet A, Trepat I, Almeda R, Saló V, Saiz E, Movilla JI, Alcaraz M, Yebra L Simó R (2008)
999 Impact of micro- And nanograzers on phytoplankton assessed by standard and size-
1000 fractionated dilution grazing experiments. Aquat Microb Ecol 50:145–156.
1001 https://doi.org/10.3354/ame01171

Online ISSN 2005-7172
Print ISSN 1738-5261

Callieri C, Stockner JG (2002) Freshwater autotrophic picoplankton: a review. J Limnol 61:1. https://doi.org/10.4081/jlimnol.2002.1

Caroppo C, Roselli L, Di Leo A (2018) Hydrological conditions and phytoplankton community in the Lesina lagoon (southern Adriatic Sea, Mediterranean). Environ Sci Pollut Res 25:1784–1799. https://doi.org/10.1007/s11356-017-0599-5

Caroppo C, Stabili L, Aresta M, Corinaldesi C, Danovaro R (2006) Impact of heavy metals and PCBs on marine picoplankton. Environ Toxicol 21:541–551. https://doi.org/10.1002/tox.20215

Casotti R, Landolfi A, Brunet C, D'Ortenzio F, Mangoni O, Ribera d'Alcalà M, Denis M (2003) Composition and dynamics of the phytoplankton of the Ionian Sea (eastern Mediterranean). J Geophys Res Oceans 108:. https://doi.org/10.1029/2002JC001541

Cerino F, Bernardi Aubry F, Coppola J, et al (2012) Spatial and temporal variability of pico-, nano- and microphytoplankton in the offshore waters of the southern Adriatic Sea (Mediterranean Sea). Cont Shelf Res 44:94–105. https://doi.org/10.1016/j.csr.2011.06.006

Cermeño P, Marañón E, Pérez V, Serret P, Fernández E, Castroc CG (2006) Phytoplankton size structure and primary production in a highly dynamic coastal ecosystem (Ría de Vigo, NW-Spain): Seasonal and short-time scale variability. Estuar Coast Shelf Sci 67:251–266. https://doi.org/10.1016/j.ecss.2005.11.027

Chen D, Guo C, Yu L, Lu Y, Sun J (2020) Phytoplankton growth and microzooplankton grazing in the central and northern South China Sea in the spring intermonsoon season of 2017. Acta Oceanol Sin 39:84–95. https://doi.org/10.1007/s13131-020-1593-1

Christaki U, Van Wambeke F, Lefevre D, Lagaria A, Prieur L, Pujo-Pay M, Grattepanche JD , Colombet J, Psarra S, Dolan JR, Sime-Ngando T, Conan P, Weinbauer MG, and Moutin T (2011) Microbial food webs and metabolic state across oligotrophic waters of the Mediterranean Sea during summer. Biogeosciences 8:1839–1852. https://doi.org/10.5194/bg-8-1839-2011

Cibic T, Cerino F, Karuza A, Fornasaro D, Comici C, Cabrini M (2018) Structural and functional response of phytoplankton to reduced river inputs and anomalous physical-chemical conditions in the Gulf of Trieste (northern Adriatic Sea). Science of The Total Environment 636:838–853. https://doi.org/10.1016/j.scitotenv.2018.04.205

Ciglenečki I, Vilibić I, Dautović J, Vojvodić V, Ćosović B, Zemunik P, Mihanović H (2020) Dissolved organic carbon and surface active substances in the northern Adriatic Sea: Long-term trends, variability and drivers. Sci Total Environ 730:139104. https://doi.org/10.1016/j.scitotenv.2020.139104

Corradino GL, Schnetzer A (2022) Grazing of a heterotrophic nanoflagellate on prokaryote and eukaryote prey: ingestion rates and gross growth efficiency. Mar Ecol Prog Ser 682:65–77. https://doi.org/10.3354/meps13921

Courboulès J, Vidussi F, Soulié T, Mas S, Pecqueur D, Mostajir B (2021) Effects of experimental warming on small phytoplankton, bacteria and viruses in autumn in the Mediterranean coastal Thau Lagoon. Aquat Ecol 55:647–666. https://doi.org/10.1007/s10452-021-09852-7

Online ISSN 2005-7172
Print ISSN 1738-5261

D'Alcalà MR, Conversano F, Corato F, Licandro P, Mangoni O, Marino D, Mazzocchi MG, Modigh M, Montresor M, Nardella M, Saggiomo V, Sarno D, Zingone A (2004) Seasonal patterns in plankton communities in a pluriannual time series at a coastal Mediterranean site (Gulf of Naples): an attempt to discern recurrences and trends. Sci Mar 68:65–83. https://doi.org/10.3989/scimar.2004.68s165

D'Alelio D, Russo L, Del Gaizo G, Caputi L (2022) Plankton under Pressure: How Water Conditions Alter the Phytoplankton–Zooplankton Link in Coastal Lagoons. Water 14:974. https://doi.org/10.3390/w14060974

Dam HG, Peterson WT (1988) The effect of temperature on the gut clearance rate constant of planktonic copepods. J Exp Mar Biol Ecol 123:1–14. https://doi.org/10.1016/0022-0981(88)90105-0

Decembrini F, Caroppo C, Azzaro M (2009) Size structure and production of phytoplankton community and carbon pathways channelling in the Southern Tyrrhenian Sea (Western Mediterranean). Deep Sea Res Part II Top Stud Oceanogr 56:687–699. https://doi.org/10.1016/j.dsr2.2008.07.022

Decembrini F, Caroppo C, Bergamasco A (2020) Influence of lateral advection on phytoplankton size-structure and composition in a Mediterranean coastal area. Continental Shelf Research 209:104216. https://doi.org/10.1016/j.csr.2020.104216

Decembrini F, Caroppo C, Caruso G, Bergamasco A (2021) Linking Microbial Functioning and Trophic Pathways to Ecological Status in a Coastal Mediterranean Ecosystem. Water 13:1325. https://doi.org/10.3390/w13091325

Dokulil MT, Qian K (2021) Photosynthesis, carbon acquisition and primary productivity of phytoplankton: a review dedicated to Colin Reynolds. Hydrobiologia 848:77–94. https://doi.org/10.1007/s10750-020-04321-y

Dolan JR, Pierce RW, Yang EJ, Kim SY (2012) Southern Ocean Biogeography of Tintinnid Ciliates of the Marine Plankton. J Eukaryot Microbiol 59:511–519. https://doi.org/10.1111/j.1550-7408.2012.00646.x

Dong Y, Li QP, Wu Z, Shuai Y, Liu Z, Ge Z, Zhou W, Chen Y (2021) Biophysical controls on seasonal changes in the structure, growth, and grazing of the size-fractionated phytoplankton community in the northern South China Sea. Biogeosciences 18:6423–6434. https://doi.org/10.5194/bg-18-6423-2021

Dopheide A, Lear G, Stott R, Lewis G (2011) Preferential Feeding by the Ciliates Chilodonella and Tetrahymena spp. and Effects of These Protozoa on Bacterial Biofilm Structure and Composition. Appl Environ Microbiol 77:4564–4572. https://doi.org/10.1128/AEM.02421-10

Drira Z, Bel Hassen M, Ayadi H, Aleya L (2014) What factors drive copepod community distribution in the Gulf of Gabes, Eastern Mediterranean Sea? Environ Sci Pollut Res 21:2918–2934. https://doi.org/10.1007/s11356-013-2250-4

Drira Z, Chaari D, Hamza A, Hassen MB, Pagano M, Ayadi H (2017) Diazotrophic cyanobacteria signatures and their relationship to hydrographic conditions in the Gulf of Gabes, Tunisia. J Mar Biol Assoc U K 97:69–80. https://doi.org/10.1017/S0025315415002210

Online ISSN 2005-7172
Print ISSN 1738-5261

Drira Z, Hamza A, Belhassen M, Ayadi H, Bouaïn A, Aleya L (2008) Dynamics of dinoflagellates and environmental factors during the summer in the Gulf of Gabes (Tunisia, Eastern Mediterranean Sea). Sci Mar 72:59–71. https://doi.org/10.3989/scimar.2008.72n159

Drira Z, Hassen MB, Hamza A, Rebai A, Bouain A, Ayadi H, Aleya L (2009) Spatial and temporal variations of microphytoplankton composition related to hydrographic conditions in the Gulf of Gabès. J Mar Biol Assoc U K 89:1559–1569. https://doi.org/10.1017/S002531540900023X

Drira Z, Kmiha-Megdiche S, Sahnoun H, Hammami A, Allouche N, Tedetti M, Ayadi H, (2016) Assessment of anthropogenic inputs in the surface waters of the southern coastal area of Sfax during spring (Tunisia, Southern Mediterranean Sea). Mar Pollut Bull 104:355–363. https://doi.org/10.1016/j.marpolbul.2016.01.035

Du Yoo Y, Jeong HJ, Kim MS, Kang NS, Song JY, Shin W, Lee K (2009) Feeding by Phototrophic Red-Tide Dinoflagellates on the Ubiquitous Marine Diatom Skeletonema costatum. J Eukaryot Microbiol 56:413–420. https://doi.org/10.1111/j.1550-7408.2009.00421.x

Duarte CM, Agustí S, Agawin NSR (2000) Response of a Mediterranean phytoplankton community to increased nutrient inputs: a mesocosm experiment. Mar Ecol Prog Ser 195:61–70. https://doi.org/10.3354/meps195061

El Kateb A, Stalder C, Rüggeberg A, Neururer C, Spangenberg JE, Spezzaferri S (2018) Impact of industrial phosphate waste discharge on the marine environment in the Gulf of Gabes (Tunisia). PloS one, 13(5), e0197731. https://doi.org/10.1371/journal.pone.0197731

Estrada M, Varela RA, Salat J, Cruzado A, Arias E (1999) Spatio-temporal variability of the winter phytoplankton distribution across the Catalan and North Balearic fronts (NW Mediterranean). J Plankton Res 21:1–20. https://doi.org/10.1093/plankt/21.1.1

Feki-Sahnoun W, Hamza A, Njah H, Barrajd N, Mahfoudia M, Rebaie A, Bel Hassen M (2017) A Bayesian network approach to determine environmental factors controlling Karenia selliformis occurrences and blooms in the Gulf of Gabès, Tunisia. Harmful Algae 63:119–132. https://doi.org/10.1016/j.hal.2017.01.013

Ferland J, Gosselin M, Starr M (2011) Environmental control of summer primary production in the Hudson Bay system: The role of stratification. J Mar Syst 88:385–400. https://doi.org/10.1016/j.jmarsys.2011.03.015

Gaudy R, Youssara F, Diaz F, Raimbault P (2003) Biomass, metabolism and nutrition of zooplankton in the Gulf of Lions (NW Mediterranean). Oceanologica Acta, 26(4): 357-372.https://doi:10.1016/S0399-1784(03)00016-1

Geyer NL, Huettel M, Wetz MS (2018) Phytoplankton Spatial Variability in the River-Dominated Estuary, Apalachicola Bay, Florida. Estuaries and Coasts, 41(7), 2024-2038. https://doi.org/10.1007/s12237-018-0402-y

Giannakourou A, Tsiola A, Kanellopoulou M, Magiopoulos I, Siokou I, Pitta P (2014) Temporal variability of the microbial food web (viruses to ciliates) under the influence of the Black Sea Water inflow (N. Aegean, E. Mediterranean). Mediterr Mar Sci 769–780. https://doi.org/10.12681/mms.1041

Online ISSN 2005-7172
Print ISSN 1738-5261

Girault M, Arakawa H, Hashihama F (2013) Phosphorus stress of microphytoplankton community in the western subtropical North Pacific. Journal of plankton research, 35(1), 146-157. https://doi.org/10.1093/plankt/fbs076

Grami B, Niquil N, Sakka Hlaili A, Gosselin M, Hamel D, Hadj Mabrouk H (2008) The plankton food web of the Bizerte Lagoon (South-western Mediterranean): II. Carbon steady-state modelling using inverse analysis. Estuar Coast Shelf Sci 79:101–113. https://doi.org/10.1016/j.ecss.2008.03.009

Grattepanche JD, Vincent D, Breton E, Christaki U (2011) Microzooplankton herbivory during the diatom–Phaeocystis spring succession in the eastern English Channel. J Exp Mar Biol Ecol 404:87–97. https://doi.org/10.1016/j.jembe.2011.04.004

Grinienė E, Šulčius S, Kuosa H (2016) Size-selective microzooplankton grazing on the phytoplankton in the Curonian Lagoon (SE Baltic Sea). Oceanologia 58:292–301. https://doi.org/10.1016/j.oceano.2016.05.002

Gueroun SM, Molinero JC, Piraino S, Dali Yahia MN (2020) Population dynamics and predatory impact of the alien jellyfish Aurelia solida (Cnidaria, Scyphozoa) in the Bizerte Lagoon (southwestern Mediterranean Sea). Mediterr Mar Sci 21:22–35. doi: https://doi.org/10.12681/mms.17358

Halouani G, Abdou K, Hattab T, Romdhane MS, Lasram FBR, Le Loc'h F (2016) A spatio-temporal ecosystem model to simulate fishing management plans: A case of study in the Gulf of Gabes (Tunisia). Mar Policy 69:62–72. https://doi.org/10.1016/j.marpol.2016.04.002

Hamdi I, Denis M, Bellaaj-Zouari A, et al (2015) The characterisation and summer distribution of ultraphytoplankton in the Gulf of Gabès (Eastern Mediterranean Sea, Tunisia) by using flow cytometry. Cont Shelf Res 93:27–38. https://doi.org/10.1016/j.csr.2014.10.002

Hannachi I, Drira Z, Belhassen M, Hamza A, Ayadi H, Bouain A, Aleya L (2008) Abundance and Biomass of the Ciliate Community during a Spring Cruise in the Gulf of Gabes (Eastern Mediterranean Sea, Tunisia). Acta Protozool 14

Hargraves PE (2002) The ebridian flagellates Ebria and Hermesinum. Plankton Biology and Ecology, 49(1), 9-16.

Hattour MJ, Sammari C, Ben Nassrallah S (2010) Hydrodynamique du golfe de Gabès déduite à partir des observations de courants et de niveaux. Rev Paralia 3:3.1-3.12. https://doi.org/10.5150/revue-paralia.2010.003

He X, Wang Z, Bai Z, Han L, Chen M (2021) Diel Feeding Rhythm and Grazing Selectivity of Small-Sized Copepods in a Subtropical Embayment, the Northern South China Sea. Front Mar Sci 8: 611. https://doi.org/10.3389/fmars.2021.658664

Hillebrand H, Dürselen CD, Kirschtel D, Pollingher U, Zohary T (1999) Biovolume Calculation for Pelagic and Benthic Microalgae. J Phycol 35:403–424. https://doi.org/10.1046/j.1529-8817.1999.3520403.x

Online ISSN 2005-7172
Print ISSN 1738-5261

Horn HG, Boersma M, Garzke J, Sommer U, Aberle N (2020) High CO2 and warming affect microzooplankton food web dynamics in a Baltic Sea summer plankton community. Mar Biol 167:69. https://doi.org/10.1007/s00227-020-03683-0

Irigoien X (1998) Gut clearance rate constant, temperature and initial gut contents: a review. J Plankton Res 20:997–1003. https://doi.org/10.1093/plankt/20.5.997

Jafari F, Ramezanpour Z, Sattari M (2015) First record of Ebria tripartita (Schumann) Lemmermann, 1899 from south of the Caspian Sea. Casp J Environ Sci 13:283–288

Jeong HJ, Yoo YD, Kang NS, Rho JR, Seong KA, Park JW, Yih W (2010) Ecology of Gymnodinium aureolum. I. Feeding in western Korean waters. Aquat Microb Ecol 59:239–255. https://doi.org/10.3354/ame01394

Jyothibabu R, Vinayachandran PN, Madhu NV, Robinc RS, Karnan C, Jagadeesan L, Anjusha A (2015) Phytoplankton size structure in the southern Bay of Bengal modified by the Summer Monsoon Current and associated eddies: Implications on the vertical biogenic flux. Journal of Marine Systems 143:98–119. https://doi.org/10.1016/j.jmarsys.2014.10.018

Kase L, Metfies K, Kraberg AC, Neuhaus S, Meunier CL, Wiltshire KH, Boersma M (2021) Metabarcoding analysis suggests that flexible food web interactions in the eukaryotic plankton community are more common than specific predator–prey relationships at Helgoland Roads, North Sea. ICES J Mar Sci 78:3372–3386. https://doi.org/10.1093/icesjms/fsab058

Katechakis A, Stibor H, Sommer U, Hansen T (2004) Feeding selectivities and food niche separation of Acartia clausi, Penilia avirostris (Crustacea) and Doliolum denticulatum (Thaliacea) in Blanes Bay (Catalan Sea, NW Mediterranean). J Plankton Res 26:589–603. https://doi.org/10.1093/plankt/fbh062

Kchaou N, Elloumi J, Drira Z, Hamza A, Ayadi H, Bouain A, Aleya L (2009) Distribution of ciliates in relation to environmental factors along the coastline of the Gulf of Gabes, Tunisia. Estuar Coast Shelf Sci 83:414–424. https://doi.org/10.1016/j.ecss.2009.04.019

Khammeri Y, Hamza IS, Zouari AB, Hamza A, Sahli E, Akrout F, Hassen MB (2018) Atmospheric bulk deposition of dissolved nitrogen, phosphorus and silicate in the Gulf of Gabès (South Ionian Basin); implications for marine heterotrophic prokaryotes and ultraphytoplankton; implications for marine heterotrophic prokaryotes and ultraphytoplankton. Continental Shelf Research, 2018, vol. 159, p. 1-11. https://doi.org/10.1016/j.csr.2018.03.003

Khammeri Y, Bellaaj-Zouari A, Hamza A, Medhioub W, Sahli E, Akrout F, Barraj N, Ben Kacem MY, Bel Hassen M(2020) Ultraphytoplankton community composition in Southwestern and Eastern Mediterranean Basin: Relationships to water mass properties and nutrients. Journal of Sea Research 158:101875. https://doi.org/10.1016/j.seares.2020.101875

Khedhri I, Lavesque N, Bonifácio P, Djabou H, Afli A (2014) First record of Naineris setosa (Verrill, 1900) (Annelida: Polychaeta: Orbiniidae) in the Western Mediterranean Sea. BioInvasions Rec 3:83–88. https://doi.org/10.3391/bir.2014.3.2.05

Online ISSN 2005-7172
Print ISSN 1738-5261

Kleppel GS, Pieper RE (1984) Phytoplankton pigments in the gut concents of planktonic copepods from coastal waters off southern California. Mar Biol 78:193–198. https://doi.org/10.1007/BF00394700

Kojima D, Hamao Y, Amei K, Fukai Y, Matsuno K, Mitani Y, Yamaguchi A (2022) Vertical distribution, standing stocks, and taxonomic accounts of the entire plankton community, and the estimation of vertical material flux via faecal pellets in the southern Okhotsk Sea. Deep Sea Res Part Oceanogr Res Pap 185:103771. https://doi.org/10.1016/j.dsr.2022.103771

Kovač Ž, Platt T, Ninčević Gladan Ž, Morović M, Sathyendranath S, Raitsos DE, Veža J (2018) A 55-Year Time Series Station for Primary Production in the Adriatic Sea: Data Correction, Extraction of Photosynthesis Parameters and Regime Shifts. https://www.mdpi.com/2072-4292/10/9/1460.

Landry MR, Hassett RP (1982) Estimating the grazing impact of marine micro-zooplankton. Mar Biol 67:283–288. https://doi.org/10.1007/BF00397668

Landry MR, Swalethorp R (2021) Mesozooplankton biomass, grazing and trophic structure in the bluefin tuna spawning area of the oceanic Gulf of Mexico. Journal of Plankton Research fbab008. https://doi.org/10.1093/plankt/fbab008

Laurenceau-Cornec EC, Trull TW, Davies DM, Bray SG, Doran J, Planchon F, Carlotti F Jouandet MP, Cavagna AJ, Waite AM, Blain S (2015) The relative importance of phytoplankton aggregates and zooplankton fecal pellets to carbon export: insights from free-drifting sediment trap deployments in naturally iron-fertilised waters near the Kerguelen Plateau. Biogeosciences 12:1007–1027. https://doi.org/10.5194/bg-12-1007-2015

Leblanc K, Quéguiner B, Diaz F, Cornet V, Michel-Rodriguez M, Durrieu de Madron X, Bowler C, Malviya S, Thyssen M, Grégori G, Rembauville M, Grosso O, Poulain J, de Vargas C, Pujo-Pay M, Conan P (2018) Nanoplanktonic diatoms are globally overlooked but play a role in spring blooms and carbon export. Nat Commun 9:953. https://doi.org/10.1038/s41467-018-03376-9

Legendre and Le Fèvre L (1989) Hydrodynamical singularities as controls of recycled versus export production in oceans. In: Berger W.H., Smetacek V.S. and Wefer G. (ed.) Product Ocean Present Pasts, John Wiley and sons Limited, Dahlem, 49-63.

Legendre L, Rassoulzadegan F (1996) Food-web mediated export of biogenic carbon in oceans:hydrodynamic control. Mar Ecol Prog Ser 145:179–193. https://doi.org/10.3354/meps145179

Legendre L, Rassoulzadegan F (1995) Plankton and nutrient dynamics in marine waters. Ophelia 41:153–172. https://doi.org/10.1080/00785236.1995.10422042

Leruste A, Pasqualini V, Garrido M, Malet N, De Wit R, Bec B (2019) Physiological and behavioral responses of phytoplankton communities to nutrient availability in a disturbed Mediterranean coastal lagoon. Estuar Coast Shelf Sci 219:176–188. https://doi.org/10.1016/j.ecss.2019.02.014

Online ISSN 2005-7172
Print ISSN 1738-5261

Li Q, Edwards KF, Schvarcz CR, Steward GF (2022) Broad phylogenetic and functional diversity among mixotrophic consumers of Prochlorococcus. ISME J 16:1557–1569. https://doi.org/10.1038/s41396-022-01204-z

Liu Q, Chai F, Dugdale R, Chao Y, Xue H, Rao S, Zhang Y (2018) San Francisco Bay nutrients and plankton dynamics as simulated by a coupled hydrodynamic-ecosystem model. Cont Shelf Res 161:29–48. https://doi.org/10.1016/j.csr.2018.03.008

Livanou E, Lagaria A, Santi I, Mandalakis M, Pavlidou A, Lika K, Psarra S, (2019) Pigmented and heterotrophic nanoflagellates: Abundance and grazing on prokaryotic picoplankton in the ultra-oligotrophic Eastern Mediterranean Sea. Deep Sea Res Part II Top Stud Oceanogr 164:100–111. https://doi.org/10.1016/j.dsr2.2019.04.007

Lund, C. Kipling, E. D. Le Cren (1958) The inverted microscope method of estimating algal numbers and the statistical basis of estimations by counting. . Hydrobiologia. 11, 143-170. https://doi.org/10.1007/BF00007865

Makhlouf Belkahia N, Pagano M, Chevalier C, Devenon JL, Yahia MND (2021) Zooplankton abundance and community structure driven by tidal currents in a Mediterranean coastal lagoon (Boughrara, Tunisia, SW Mediterranean Sea). Estuar Coast Shelf Sci 250:107101. https://doi.org/10.1016/j.ecss.2020.107101

Mansano AS, Hisatugo KF, Hayashi LH, Regali-Seleghim MH (2014) The importance of protozoan bacterivory in a subtropical environment (Lobo-Broa Reservoir, SP, Brazil). Braz J Biol 74:569–578. https://doi.org/10.1590/bjb.2014.0081

Mansouri B, Gzam M, Souid F, Telahigue F, Chahlaoui A, Ouarrak K, Kharroubi A, (2020) Assessment of heavy metal contamination in Gulf of Gabès coastland (southeastern Tunisia): impact of chemical industries and drift currents. Arab J Geosci 13:1180. https://doi.org/10.1007/s12517-020-06163-3

Margalef R (1978) Life-forms of phytoplankton as survival alternatives in an unstable environment. Ocean Acta 1:493–509

Marques F, Chainho P, Costa JL, Domingos I, Angélico MM (2015) Abundance, seasonal patterns and diet of the non-native jellyfish Blackfordia virginica in a Portuguese estuary. Estuar Coast Shelf Sci 167:212–219. https://doi.org/10.1016/j.ecss.2015.07.024

Marquis E, Niquil N, Delmas D, Hartmann HJ, Bonnet D, Carlotti F, Dupuy C (2007) Inverse analysis of the planktonic food web dynamics related to phytoplankton bloom development on the continental shelf of the Bay of Biscay, French coast. Estuar Coast Shelf Sci 73:223–235. https://doi.org/10.1016/j.ecss.2007.01.003

Martin-Cereceda M, Novarino G, Young JR (2003) Grazing by Prymnesium parvum on small planktonic diatoms. Aquat Microb Ecol 33:191–199. https://doi.org/10.3354/ame033191

Masclaux H, Tortajada S, Philippine O, Robin FX, Dupuy C (2015) Planktonic food web structure and dynamic in freshwater marshes after a lock closing in early spring. Aquat Sci 77:115–128. https://doi.org/10.1007/s00027-014-0376-1

Online ISSN 2005-7172
Print ISSN 1738-5261

Mauchline (1998) Adv. Mar. Biol. 33: The biology of calanoid copepods. Volume 33 - 1st Edition.

Mayot N, D'Ortenzio F, Taillandier V, Prieur L, De Fommervault OP, Claustre H, Conan P (2017) Physical and Biogeochemical Controls of the Phytoplankton Blooms in North Western Mediterranean Sea: A Multiplatform Approach Over a Complete Annual Cycle (2012–2013 DEWEX Experiment). J Geophys Res Oceans 122:9999–10019. https://doi.org/10.1002/2016JC012052

Mayot N, Nival P, Levy M (2020) Primary Production in the Ligurian Sea. The Mediterranean Sea in the Era of Global Change 1: 30 Years of Multidisciplinary Study of the Ligurian Sea, 139-164. https://doi.org/10.1002/9781119706960.ch6

Meddeb M, Grami B, Chaalali A, Haraldsson H, Niquil N, Pringault O, Sakka Hlaili A (2018) Plankton food-web functioning in anthropogenically impacted coastal waters (SW Mediterranean Sea): An ecological network analysis. Prog Oceanogr 162:66–82. https://doi.org/10.1016/j.pocean.2018.02.013

Meddeb M, Niquil N, Grami B, Mejri K, Haraldsson M, Chaalali A, Sakka Hlaili A (2019) A new type of plankton food web functioning in coastal waters revealed by coupling Monte Carlo Markov chain linear inverse method and ecological network analysis. Ecol Indic 104:67–85. https://doi.org/10.1016/j.ecolind.2019.04.077

MedECC (2020) Climate and Environmental Change in the Mediterranean Basin – Current Situation and Risks for the Future. First Mediterranean Assessment Report [Cramer W, Guiot, J, Marini, K, [eds.]] Union for Mediterranean, Plan Bleu, UNEP/MAP, Marseille, France, 632pp. ISBN: 978-2-9577416-0-1/ DOI : 10.5281/zenodo.4768833

Menden-Deuer S, Lessard EJ (2000) Carbon to volume relationships for dinoflagellates, diatoms, and other protist plankton. Limnol Oceanogr 45:569–579. https://doi.org/10.4319/lo.2000.45.3.0569

Moigis and Gocke (2003) Primary production of phytoplankton estimated by means of the dilution method in coastal waters. Journal of Plankton Research. 25: 10. doi: 10.1093/plankt/fbg089,

Morales CE, Harris RP, Head RN, Tranter PRG (1993) Copepod grazing in the oceanic northeast Atlantic during a 6 week drifting station: the contribution of size classes and vertical migrants. Journal of Plankton Research 15:185–212. https://doi.org/10.1093/plankt/15.2.185

Moran XAG, Estrada M (2001) Short-term variability of photosynthetic parameters and particulate and dissolved primary production in the Alboran Sea (SW Mediterranean). Mar Ecol Prog Ser 212:53–67. https://doi.org/10.3354/meps212053

Morsy A, Ebeid M, Soliman A, Halim AA, Ali AE, Fahmy M (2022) Evaluation of the water quality and the eutrophication risk in Mediterranean sea area: A case study of the Port Said Harbour, Egypt. Environ Chall 7:100484. https://doi.org/10.1016/j.envc.2022.100484

Online ISSN 2005-7172
Print ISSN 1738-5261

Negrete-García G, Luo JY, Long MC, Lindsay K, Levy M, Barton AD (2022) Plankton energy flows using a global size-structured and trait-based model. bioRxiv. https://doi.org/10.1101/2022.02.01.478546

Olson MB, Strom SL (2002) Phytoplankton growth, microzooplankton herbivory and community structure in the southeast Bering Sea: insight into the formation and temporal persistence of an Emiliania huxleyi bloom. Deep Sea Res Part II Top Stud Oceanogr 49:5969–5990. https://doi.org/10.1016/S0967-0645(02)00329-6

Othmani A, Béjaoui B, Chevalier C, Elhmaidi D, Devenon JL, Aleya L (2017) High-resolution numerical modelling of the barotropic tides in the Gulf of Gabes, eastern Mediterranean Sea (Tunisia). J Afr Earth Sci 129:224–232. https://doi.org/10.1016/j.jafrearsci.2017.01.007

Paklar GB, Vilibić I, Grbec B, Matić F, Mihanović H, Džoić T, Kušpilić G (2020) Record-breaking salinities in the middle Adriatic during summer 2017 and concurrent changes in the microbial food web. Progress in Oceanography 185: 102345. https://doi.org/10.1016/j.pocean.2020.102345

Parsons TR, Harrison PJ, Acreman JC, Dovey HM, Thompson PA, Lalli CM, Xiaolin C (1984) An experimental marine ecosystem response to crude oil and Corexit 9527: Part 2—biological effects. Marine Environmental Research 13(4), 265-275. https://doi.org/10.1016/0141-1136(84)90033-3

Pecqueur D, Courboulès J, Roques C, Mas S, Pete R, Vidussi F, Mostajir B (2022) Simultaneous Study of the Growth and Grazing Mortality Rates of Microbial Food Web Components in a Mediterranean Coastal Lagoon. Diversity, 14(3), 186.https://www.mdpi.com/1424-2818/14/3/186.

Peters F, Arin L, Marrasé C, Berdalet E, Sala MM (2006) Effects of small-scale turbulence on the growth of two diatoms of different size in a phosphorus-limited medium. J Mar Syst 61:134–148. https://doi.org/10.1016/j.jmarsys.2005.11.012

Psarra S, Zohary T, Krom MD, Mantoura RFC, Polychronaki T, Stambler N, Thingstad TF (2005). Phytoplankton response to a Lagrangian phosphate addition in the Levantine Sea (Eastern Mediterranean). Deep Sea Research Part II: Topical Studies in Oceanography, 52(22-23), 2944-2960. https://doi.org/10.1016/j.dsr2.2005.08.015

Putt M, Stoecker DK (1989) An experimentally determined carbon : volume ratio for marine "oligotrichous" ciliates from estuarine and coastal waters. Limnol Oceanogr 34:1097–1103. https://doi.org/10.4319/lo.1989.34.6.1097

Raimbault P, Garcia N, Cerutti F (2008) Distribution of inorganic and organic nutrients in the South Pacific Ocean − evidence for long-term accumulation of organic matter in nitrogen-depleted waters. Biogeosciences 5:281–298. https://doi.org/10.5194/bg-5-281-2008

Rassoulzadegan F, Laval-Peuto M, Sheldon RW (1988) Partitioning of the food ration of marine ciliates between pico- and nanoplankton. Hydrobiologia, 159(1), 75-88. https://doi.org/10.1007/BF00007369

Online ISSN 2005-7172
Print ISSN 1738-5261

Raveh O, David N, Rilov G, Rahav E (2015) The Temporal Dynamics of Coastal Phytoplankton and Bacterioplankton in the Eastern Mediterranean Sea. PloS one, 10(10), e0140690. https://doi.org/10.1371/journal.pone.0140690

Rekik A, Denis M, Maalej S, Ayadi H (2015) Spatial and seasonal variability of pico-, nano- and microphytoplankton at the bottom seawater in the north coast of Sfax, Eastern Mediterranean Sea. Environ Sci Pollut Res 22:15961–15975. https://doi.org/10.1007/s11356-015-4811-1

Rekik A, Kmiha-Megdiche S, Drira Z, Pagano M, Ayadi H, Zouari AB, Elloumi J (2021) Spatial variations of planktonic ciliates, predator-prey interactions and their environmental drivers in the Gulf of Gabes-Boughrara lagoon system. Estuar Coast Shelf Sci 254:107315. https://doi.org/10.1016/j.ecss.2021.107315

Riccardi N (2010) Selectivity of plankton nets over mesozooplankton taxa: implications for abundance, biomass and diversity estimation. J Limnol 69:287. https://doi.org/10.4081/jlimnol.2010.287

Ross ON, Fraysse M, Pinazo C, Pairaud I (2016) Impact of an intrusion by the Northern Current on the biogeochemistry in the eastern Gulf of Lion, NW Mediterranean . Estuarine, Coastal and Shelf Science 170: 1-9. https://doi.org/10.1016/j.ecss.2015.12.022

Saiz E, Rodriguez V, Alcaraz M (1992) Spatial distribution and feeding rates of Centropages typicus in relation to frontal hydrographic structures in the Catalan Sea (Western Mediterranean). Mar Biol 112:49–56. https://doi.org/10.1007/BF00349727

Sakka Hlaili A, Grami B, Hadj Mabrouk H, Gosselin M, Hamel D (2007) Phytoplankton growth and microzooplankton grazing rates in a restricted Mediterranean lagoon (Bizerte Lagoon, Tunisia). Mar Biol 151:767–783. https://doi.org/10.1007/s00227-006-0522-y

Sakka Hlaili A, Grami B, Niquil N, Gosselin M, Hamel D, Troussellier M, Mabrouk H (2008) The planktonic food web of the Bizerte lagoon (south-western Mediterranean) during summer: I. Spatial distribution under different anthropogenic pressures. Estuar Coast Shelf Sci 78:61–77. https://doi.org/10.1016/j.ecss.2007.11.010

Sakka Hlaili AS, Niquil N, Legendre L (2014) Planktonic food webs revisited: Reanalysis of results from the linear inverse approach. Prog Oceanogr 120:216–229. https://doi.org/10.1016/j.pocean.2013.09.003

Salgado-Hernanz PM, Racault M-F, Font-Muñoz JS, Basterretxea G (2019) Trends in phytoplankton phenology in the Mediterranean Sea based on ocean-colour remote sensing. Remote Sens Environ 221:50–64. https://doi.org/10.1016/j.rse.2018.10.036

Sammari C, Koutitonsky VG, Moussa M (2006) Sea level variability and tidal resonance in the Gulf of Gabes, Tunisia. Continental Shelf Research 26:338–350. https://doi.org/10.1016/j.csr.2005.11.006

Sautour B, Artigas LF, Delmas D, Herbland A, Laborde P (2000) Grazing impact of micro- and mesozooplankton during a spring situation in coastal waters off the Gironde estuary. J Plankton Res 22:531–552. https://doi.org/10.1093/plankt/22.3.531

Online ISSN 2005-7172
Print ISSN 1738-5261

Seong KA, Jeong HJ, Kim S, Kim GH, Kang JH (2006) Bacterivory by co-occurring red-tide algae, heterotrophic nanoflagellates, and ciliates. Mar Ecol Prog Ser 322:85–97. https://doi.org/10.3354/meps322085

Sherr EB, Sherr BF (1993) Preservation and Storage of Samples for Enumeration of Heterotrophic Protists. In: Handbook of Methods in Aquatic Microbial Ecology. CRC Press

Sherr EB, Sherr BF (2007) Heterotrophic dinoflagellates: a significant component of microzooplankton biomass and major grazers of diatoms in the sea. Mar Ecol Prog Ser 352:187–197. https://doi.org/10.3354/meps07161

Shinada A, Ikeda T, Ban S, Tsuda A (2000) Seasonal changes in micro-zooplankton grazing on phytoplankton assemblages in the Oyashio region. Plankton Biol. Ecol. 47(2), 85-92.

Siokou-Frangou I, Christaki U, Mazzocchi MG, Montresor M, Ribera d'Alcalá M, Vaqué D, Zingone A (2010) Plankton in the open Mediterranean Sea: a review. Biogeosciences 7:1543–1586. https://doi.org/10.5194/bg-7-1543-2010

Slaughter AM, Bollens SM, Bollens GR (2006) Grazing impact of mesozooplankton in an upwelling region off northern California, 2000–2003. Deep Sea Res Part II Top Stud Oceanogr 53:3099–3115. https://doi.org/10.1016/j.dsr2.2006.07.005

Smith VH, Joye SB, Howarth RW (2006) Eutrophication of freshwater and marine ecosystems. Limnol Oceanogr 51:351–355. https://doi.org/10.4319/lo.2006.51.1_part_2.0351

Šolić M, Krstulović N, Kušpilić G, Ninčević Gladan Ž, Bojanić N, Šestanović S, Šantić D, Ordulj M (2010) Changes in microbial food web structure in response to changed environmental trophic status: A case study of the Vranjic Basin (Adriatic Sea). Marine Environmental Research 70:239–249. https://doi.org/10.1016/j.marenvres.2010.05.007

Sorgente R, Olita A, Oddo P, Fazioli L, Ribotti A (2011) Numerical simulation and decomposition of kinetic energy in the Central Mediterranean: insight on mesoscale circulation and energy conversion. Ocean Sci 7:503–519. https://doi.org/10.5194/os-7-503-2011

Stibor H, Stockenreiter M, Nejstgaard JC, Ptacnik R, Sommer U (2019) Trophic switches in pelagic systems. Curr Opin Syst Biol 13:108–114. https://doi.org/10.1016/j.coisb.2018.11.006

Tanaka T, Zohary T, Krom MD, Law CS, Pitta P, Psarra S, Rassoulzadegan F, Thingstad TF, Tselepides A, Woodward EMS, Flaten GAF, Skjoldal EF, Zodiatis, G (2007). Microbial community structure and function in the Levantine Basin of the eastern Mediterranean. Deep Sea Research Part I: Oceanographic Research Papers, 54(10), 1721-1743. https://doi.org/10.1016/j.dsr.2007.06.008

Ter Braak (1986) Canonical Correspondence Analysis: A New Eigenvector Technique for Multivariate Direct Gradient Analysis - ter Braak - 1986 - Ecology - Wiley Online Library. https://esajournals.onlinelibrary.wiley.com/doi/abs/10.2307/1938672.

Totti C, Cangini M, Ferrari C, Kraus R, Pompei M, Pugnetti A, Romagnoli T, Vanucci S, Socal G (2005), Phytoplankton size-distribution and community structure in relation to

Online ISSN 2005-7172
Print ISSN 1738-5261

mucilage occurrence in the northern Adriatic Sea. Science of the Total Environment 353(1-3): 204-217. https://doi.org/10.1016/j.scitotenv.2005.09.028

Trombetta T, Bouget F-Y, Félix C, Mostajir B, Vidussi F (2022) Microbial Diversity in a North Western Mediterranean Sea Shallow Coastal Lagoon Under Contrasting Water Temperature Conditions. Front Mar Sci 9. https://doi.org/10.3389/fmars.2022.858744

Trombetta T, Vidussi F, Roques C, Mas S, Scotti M, Mostajir B (2021) Co-occurrence networks reveal the central role of temperature in structuring the plankton community of the Thau Lagoon. Sci Rep 11:17675. https://doi.org/10.1038/s41598-021-97173-y

Tseng LC, Kumar R, Dahms HU, Chen QC, Hwang JS (2008) Copepod Gut Contents, Ingestion Rates, and Feeding Impacts in Relation to Their Size Structure in the Southeastern Taiwan Strait. Zool Stud 15

Utermöhl (1931) Neue Wege in der quantitativen Erfassung des Plankton.(Mit besonderer Berücksichtigung des Ultraplanktons.) Mit 4 Abbildungen im Text. Internationale Vereinigung für theoretische und angewandte Limnologie: Verhandlungen, 5(2), 567-596. https://doi.org/10.1080/03680770.1931.11898492

Vargas CA, González HE (2004) Plankton community structure and carbon cycling in a coastal upwelling system. II. Microheterotrophic pathway. Aquat Microb Ecol 34:165–180. https://doi.org/10.3354/ame034165

Vargas CA, Martínez RA, Cuevas LA, Pavez MA, Cartes C, Gonza´lez HE, Escribano R, Daneri G (2007) The relative importance of microbial and classical food webs in a highly productive coastal upwelling area. Limnology and Oceanography 52:1495–1510. https://doi.org/10.4319/lo.2007.52.4.1495

Varkitzi I, Psarra S, Assimakopoulou G, et al (2020) Phytoplankton dynamics and bloom formation in the oligotrophic Eastern Mediterranean: Field studies in the Aegean, Levantine and Ionian seas. Deep Sea Res Part II Top Stud Oceanogr 171:104662. https://doi.org/10.1016/j.dsr2.2019.104662

Vascotto I, Mozetič P, Francé J (2021) Phytoplankton Time-Series in a LTER Site of the Adriatic Sea: Methodological Approach to Decipher Community Structure and Indicative Taxa. Water 13:2045. https://doi.org/10.3390/w13152045

Verity PG, Robertson CY, Tronzo CR, Andrews MG, Nelson JR, Sieracki ME (1992) Relationships between cell volume and the carbon and nitrogen content of marine photosynthetic nanoplankton. Limnol Oceanogr 37:1434–1446. https://doi.org/10.4319/lo.1992.37.7.1434

Vidussi F, Marty J-C, Chiavérini J (2000) Phytoplankton pigment variations during the transition from spring bloom to oligotrophy in the northwestern Mediterranean sea. Deep Sea Res Part Oceanogr Res Pap 47:423–445. https://doi.org/10.1016/S0967-0637(99)00097-7

Viñas MD, Negri RM, Cepeda GD, Hernández D, Silva R, Daponte MC, Capitanio FL (2013) Seasonal succession of zooplankton in coastal waters of the Argentine Sea (Southwest Atlantic Ocean): prevalence of classical or microbial food webs. Mar Biol Res 9:371–382. https://doi.org/10.1080/17451000.2012.745003

Online ISSN 2005-7172
Print ISSN 1738-5261

Ward BA, Dutkiewicz S, Jahn O, Follows MJ (2012) A size-structured food-web model for the global ocean. Limnol Oceanogr 57:1877–1891. https://doi.org/10.4319/lo.2012.57.6.1877

Wickham SA, Wenta P, Sinner A, Weiss R (2022) Microzooplankton grazing and community composition in a high-productivity marine ecosystem. J Plankton Res 44:414–426. https://doi.org/10.1093/plankt/fbac015

Xiang Y, Lam PJ, Burd AB, Hayes CT (2022) Estimating Mass Flux From Size-Fractionated Filtered Particles: Insights Into Controls on Sinking Velocities and Mass Fluxes in Recent U.S. GEOTRACES Cruises. Glob Biogeochem Cycles 36:e2021GB007292. https://doi.org/10.1029/2021GB007292

Yang J, Wei H, Yalin T, et al (2019) Combined effects of food resources and exposure to ammonium nitrogen on population growth performance in the bacterivorous ciliate Paramecium caudatum. Eur J Protistol 71:125631. https://doi.org/10.1016/j.ejop.2019.125631

Yang J, Löder MGJ, Wiltshire KH, Montagnes DJ (2022) Comparing the Trophic Impact of Microzooplankton during the Spring and Autumn Blooms in Temperate Waters . Estuaries and Coasts, 44(1), 189-198. https://doi.org/10.1007/s12237-020-00775-4

Zayen A, Sayadi S, Chevalier C, Boukthir M, Ismail SB, Tedetti M (2020) Microplastics in surface waters of the Gulf of Gabes, southern Mediterranean Sea: Distribution, composition and influence of hydrodynamics. Estuar Coast Shelf Sci 242:106832. https://doi.org/10.1016/j.ecss.2020.106832

Zhang S, Liu H, Ke Y, Li B (2017) Effect of the Silica Content of Diatoms on Protozoan Grazing. Front Mar Sci 4:202. https://doi.org/10.3389/fmars.2017.00202